

# **GTI White Paper on IMT System Operating in 6GHz Band Coexistence with Incumbents**

<http://gtigroup.org/>

**GTI**

---

# ***GTI White Paper on IMT System Operating in 6GHz Band Coexistence with Incumbents***



<b>Version:</b>	V0.0
<b>Deliverable Type</b>	<input type="checkbox"/> Procedural Document <input checked="" type="checkbox"/> Working Document
<b>Confidential Level</b>	<input checked="" type="checkbox"/> Open to GTI Operator Members <input checked="" type="checkbox"/> Open to GTI Partners <input type="checkbox"/> Open to Public
<b>Program</b>	5G eMBB
<b>Working Group</b>	Spectrum WG
<b>Project</b>	<b>Project:</b> new IMT SPECTRUM for 6GHz band
<b>Task</b>	Task-N-PM2-PJ7-2: Coexistence with incumbents
<b>Source members</b>	China Mobile, Ericsson, MediaTek, Nokia and ZTE
<b>Support members</b>	China Mobile, Ericsson, MediaTek, Nokia and ZTE
<b>Editor</b>	Chunxia Guo, Victoria Wang, Ning Li, Daoqing Qu, Junqiang Cheng, Jianhua Liu, Liyuan Zhong and Likai Hao
<b>Last Edit Date</b>	10-18-2023

---

Approval Date	
---------------	--

**Confidentiality:** This document may contain information that is confidential and access to this document is restricted to the persons listed in the Confidential Level. This document may not be used, disclosed or reproduced, in whole or in part, without the prior written authorization of GTI, and those so authorized may only use this document for the purpose consistent with the authorization. GTI disclaims any liability for the accuracy or completeness or timeliness of the information contained in this document. The information contained in this document may be subject to change without prior notice.

## Document History

---

Date	Meeting #	Version #	Revision Contents
24-8-2021			Kick Off
23-8-2022		V1.0	Draft white paper 1.0
10-03-2023		V1.1	Draft white paper 1.1
18-10-2023		V2.0	Draft white paper 2.0
17-11-2023		V2.1	Draft white paper 2.1
29-11-2023		V2.2	Draft white paper 2.2
27-12-2023		V2.3	Draft white paper 2.3 for complete version

---

## Table of Contents

1	Introduction .....	6
2	Allocation information in 6 425-7 125 MHz and in adjacent frequency bands, as appropriate 8	
3	Technical characteristics .....	9
3.1	Technical and operational characteristics of IMT systems operating in the frequency band 6 425-7 125 MHz .....	9
4	Sharing and compatibility studies .....	16
4.1	Sharing and compatibility of the fixed-satellite service (FSS) (Earth-to-space) operating in the frequency band 6 425-7 025 MHz .....	16
4.1.1	Technical characteristics .....	16
4.1.2	Channel model .....	20
4.1.3	Methodology .....	24
4.1.4	Results .....	25
4.1.5	Conclusions .....	27
4.2	Sharing and compatibility of the fixed-satellite service (FSS) (space-to-Earth) operating in the frequency band 6 700-7 075 MHz .....	27
4.2.1	Technical characteristics .....	28
4.2.2	Methodology .....	29
4.2.3	Study Results .....	32
4.2.4	Summary and analysis of the results .....	36
4.3	Sharing and compatibility of the fixed service and IMT .....	37
4.3.1	Technical characteristics .....	37
4.3.2	Methodology .....	40
4.3.3	Study results .....	41
4.3.4	Summary and analysis of the results .....	44
4.4	Sharing and compatibility of the SRS operating in the frequency band 7 145-7 190 MHz 44	
4.4.1	Technical characteristics .....	46
4.4.2	Methodology .....	47
4.4.3	Study results .....	53
4.4.4	Summary and analysis of the results .....	54
4.5	Sharing and compatibility of the SOS operating in the frequency band 7 100-7 155 ...	55

---

4.5.1	Technical characteristics.....	55
4.5.2	Methodology .....	57
4.5.3	Study results .....	59
4.5.4	Summary and analysis of the results .....	61
5	Main Discussion and Conclusion .....	63
5.1	Discussion .....	63
5.2	Conclusion.....	64
6	Abbreviation.....	65
7	References .....	66

---

# 1 Introduction

Currently, 5G is rapidly developing globally, with more than 170 countries issuing national digital strategies, and 5G has become a key enabler for social digital transformation and sustainable national economic growth. According to a report released by GSA, as of June 2021, 169 operators in 70 countries and regions around the world have opened 5G services based on 3GPP standards.

With the rapid popularization of ultra-high-definition video and XR services in the future, the traffic of 5G mobile users will continue to grow further. According to the report of ITU, by 2030, the average monthly DOU of global mobile users will reach 250GB. In addition, 5G will also be more widely used in industrial applications. Considering the above business needs, the mobile communication industry organization GSMA pointed out that by 2030, each country needs 1-2GHz intermediate frequency spectrum. The 6GHz frequency band has a good balance between coverage and capacity. Compared with other mid-frequency frequency bands, there are fewer existing services and better coexistence. Therefore, using the 6GHz frequency band for the IMT system is the key to the sustainable development of mobile communications in the next ten years.

Recently, there have been several trial tests conducted to verify the performance of the U6G system in various countries. Vodafone has made an announcement about the successful testing of the upcoming mobile spectrum in the upper 6GHz frequency band. Based on the trial test results, enabling this band for mobile use will ensure faster and more reliable 5G services for both consumers and businesses in the next 5 to 10 years. It will also prevent a shortage of mobile capacity caused by the significant increase in bandwidth demand. In addition, Telefónica Germany has also conducted trial tests on 5G using the upper 6GHz band at an established site in Stuttgart. The results were positive, showing that the band has good propagation properties in real-life scenarios. This highlights its potential value in providing indoor and outdoor coverage. While this is exciting news for digital users, it is important for mobile operators to utilize the band under appropriate conditions to fully enjoy the benefits. Overall, these trial tests have greatly advanced the industrial maturity of the U6G system.

In WRC-23, 7025-7125 MHz was successfully identified as IMT globally, and 6425-7025 MHz band was included in the identification for IMT in ITU Regions 1, Regions 2 (Brazil, Mexico) and ITU Regions 3 (Cambodia, Laos and Maldives). Almost 80% of the global population, represented by numerous countries, expressed their interest in including this band for licensed mobile services at WRC-23. Countries that failed add the footnote with IMT identification in 6425-7025MHz at this meeting may continue to apply for the identification of the 6425-7025MHz band as IMT in the form of national footnotes at subsequent WRC meetings without coexistence study. The decision by WRC-23 to harmonize the 6 GHz band across all ITU regions marks a significant milestone, offering a synchronized 6 GHz mobile coverage to billions of people. Moreover, it acts as a critical developmental trigger in the development of the 6 GHz equipment ecosystem for manufacturers.

GTI (Global TD-LTE Initiative) is an open platform advocating cooperation among global operators and vendors to energize the creation of a world-class and a growth-focused business environment, which promote a unified 5G standard and mature end-to-end ecosystem, as well

---

as explore cross-industry markets and opportunities. GTI has studied the 5G spectrum strategy to facilitate further mobile applications and demands for future development, which is very critical for GTI to start the study and preparation taking into account the world-wide spectrum development for 5G. This white paper will investigate the coexistence of IMT and existing 6GHz band services, such as FSS/FS, by exploring the models, parameters and technologies based on ITU-R agreement (R19-WP5D-C-0716!H4-N4.04!MSW-E), and timely carry out the relevant simulation to verify the theoretical analysis.

Based on the study report in this GTI report, sharing and compatibility is possible in the 6425-7125 MHz band, including urban and suburban scenarios. IMT deployments can coexist with satellite uplink. The 6425-7125 MHz band is recommended for licensed consideration, in line with the WRC-23 agenda item, which is an important extension spectrum to 5G mid band operation, particularly for outdoor urban areas and supporting 5G advanced services. Harmonization across regions simplifies device requirements. 5G Advanced products are expected from 2025, aligning with the assignment of the first U6G licenses. Future U6G deployments can exploit 700 MHz of contiguous spectrum while reusing the available 3.5 GHz site grid for citywide high-capacity coverage.

## 2 Allocation information in 6 425-7 125 MHz and in adjacent frequency bands, as appropriate

Allocation information in 6 425-7 125 MHz and in adjacent frequency bands is listed as below,

### 5 925-7 145 MHz

Allocation to services		
Region 1	Region 2	Region 3
<b>5 925-6 700</b>	FIXED 5.457 FIXED-SATELLITE (Earth-to-space) 5.457A 5.457B MOBILE 5.457C 5.149 5.440 5.458	
<b>6 700-7 075</b>	FIXED FIXED-SATELLITE (Earth-to-space) (space-to-Earth) 5.441 MOBILE 5.458 5.458A 5.458B	
<b>7 075-7 145</b>	FIXED MOBILE 5.458 5.459	
<b>7 145-7 190</b>	FIXED MOBILE SPACE RESEARCH (deep space) (Earth-to-space) 5.458 5.459	

For allocation details and footnotes text, please refer to the Radio Regulations, Edition of 2020.



---

## 3 Technical characteristics

### 3.1 Technical and operational characteristics of IMT systems operating in the frequency band 6 425-7 125 MHz

The IMT Parameters of 6 425-7 125 MHz refers to 5D/716 Chapter 4 - Annex 4.4 - Characteristics of terrestrial component of IMT for sharing and compatibility studies in preparation for WRC-23 which is finalized in ITU WP 5D #38 meeting in June 2021.

Tables 1 and 2 below provide the deployment-related parameters of IMT systems for the frequency band 6 425-7 125 MHz. Urban and Suburban macro scenarios are considered in this study. Rural is not considered in this study.

TABLE 3-1  
Deployment-related parameters for bands between 6 and 8 GHz

	Urban/suburban macro
Deployment density (Note 1)	10 BSs/km <sup>2</sup> urban / 2.4 BSs/km <sup>2</sup> suburban (Note 2, 3)
Antenna height	18 m urban / 20 m suburban
Sectorization	3 sectors
Frequency reuse	1
Indoor base station deployment	n.a.
Indoor base station penetration loss	n.a.
Below rooftop base station antenna deployment	Urban: 65% Suburban: 15%
Typical channel bandwidth	100 MHz
Network loading factor (base station load probability X%) (see Section 3.4 below and Rec. ITU-R M.2101 Annex 1, Sections 3.4.1 and 6)	50%
TDD / FDD	TDD
BS TDD activity factor	75%

Note 1: These density values are for small dense areas. For the density in satellite footprint with larger region size, section 3.3 of 5D/716 for densities in larger areas need to be considered.

Note 2: "1 BS" = 1 sector in 3-sector cell.

Note 3: This value is calculated based on use of same grid as 3-6 GHz. It is expected that the same BS infrastructure will typically be used for networks in both 3-6 GHz and 6-8 GHz. For sharing studies requiring a specific cell size, the following values should be used: 0.3 km for urban and 0.6 km for suburban.

TABLE 3-2

**UE parameters for bands between 6 and 8 GHz**

	<b>Urban/suburban macro</b>
Indoor user terminal usage	70%
Indoor user terminal penetration loss	Rec. ITU-R P.2109
User equipment density for terminals that are transmitting simultaneously (Note 1)	3 UEs per sector
UE height (Note 2)	1.5 m
Average user terminal output power	Use transmit power control
Typical antenna gain for user terminals	-4 dBi
Body loss	4 dB
UE TDD activity factor	25%
Maximum user terminal output power, PCMAX	23 dBm
Power (dBm) target value per RB, P0_PUSCH (Note 3)	-92.2
Path loss compensation factor, (same as "balancing factor" mentioned in Rec. ITU-R M.2101)	0.8

Note 1: UEs share equally the channel bandwidth, i.e. each UE is allocated 1/3 of the channel bandwidth (see Rec. ITU-R M.2101, Section 3.4.1, item 1e-f.). In sharing studies, it is assumed that the AAS BS beamforms towards each UE using the entire array

Note 2: In principle, indoor UEs are distributed over different floors of the building. It should be noted that the number of floors of buildings vary within the environment and among the countries. Moreover, the number of floors of buildings is not related to Macro BS antenna height (parameter given in the Table 1). In particular in small cities, sub-urban and rural areas, many or most of antennas are installed on masts. Therefore, for outdoor BSs, indoor UEs are assumed to be modelled on the ground floor for the sharing study.

Note 3: The target power is defined per Resource Block (RB), considering 180 kHz RB bandwidth corresponding to 15 kHz subcarrier spacing.

Implementation of AAS (see Table 3) is considered for IMT base stations in these frequency bands. Implementation of AAS is not considered in IMT user equipment / mobile stations.

TABLE 3-3

**Beamforming antenna characteristics for IMT in 6 425-10 500 MHz**

		<b>Macro suburban</b>	<b>Macro urban</b>
<b>1</b>	<b>Base station antenna characteristics</b>		
1.1	Antenna pattern	Refer to Recommendation <a href="#">ITU-R M.2101</a> Annex 1, section 5	
1.2	Element gain (dBi) (Note 1)	6.4	5.5
1.3	Horizontal/vertical 3 dB beamwidth of single element (degree)	90° for H 65° for V	90° for H 90° for V
1.4	Horizontal/vertical front-to-back ratio (dB)	30 for both H/V	30 for both H/V
1.5	Antenna polarization	Linear ±45°	Linear ±45°

		<b>Macro suburban</b>	<b>Macro urban</b>
1.6	Antenna array configuration (Row x Column) (Note 2)	16 x 8 elements	16 x 8 elements
1.7	Horizontal/Vertical radiating element spacing	0.5 of wavelength for H, 0.7 of wavelength for V	0.5 of wavelength for H, 0.5 of wavelength for V
1.8	Array Ohmic loss (dB) (Note 1)	2	2
1.9	Conducted power (before Ohmic loss) per antenna element (dBm) (Note 6)	22 (Note 5)	22 (Note 5)
1.10	Base station maximum coverage angle in the horizontal plane (degrees)	±60	±60
1.11	Base station vertical coverage range (degrees) (Notes 3, 4, 7)	90-100	90-120
1.12	Mechanical downtilt (degrees) (Note 4)	6	10

Note 1: The element gain in row 1.2 includes the loss given in row 1.8. This means that this parameter in row 1.8 is not needed for the calculation of the BS composite antenna gain and e.i.r.p.

Note 2: 16 x 8 means there are 16 vertical and 8 horizontal radiating elements.

Note 3: The vertical coverage range is given in global coordinate system, i.e. 90° being at the horizon.

Note 4: The vertical coverage range in row 1.11 includes the mechanical downtilt given in row 1.12.

Note 5: The conducted power per element assumes 16 x 8 x 2 elements (i.e. power per H/V polarized element).

Note 6: In sharing studies, the transmit power calculated using row 1.9 is applied to the typical bandwidth given in Table 1 for the corresponding frequency bands.

Note 7: In sharing studies, the UEs that are below the coverage range can be considered to be served by the "lower" bound of the electrical beam, i.e. beam steered towards the max. coverage angle. A minimum BS-UE distance along the ground of 35 m is used for urban/suburban macro environments.

The figures below present the antenna patterns used in simulation, the figures represent antenna patterns used for urban and suburban deployment scenarios, Figure 1 presents the antenna patterns in the vertical plane, Figure 2 presents the antenna patterns in the horizontal plane. Figure 3 presents the CDF of antenna gain at the interfering direction in urban scenario.

FIGURE 3-1

Vertical plane antenna radiation patterns for urban and suburban scenarios

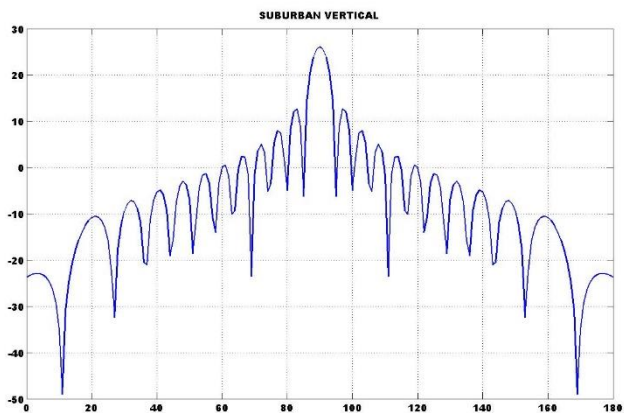
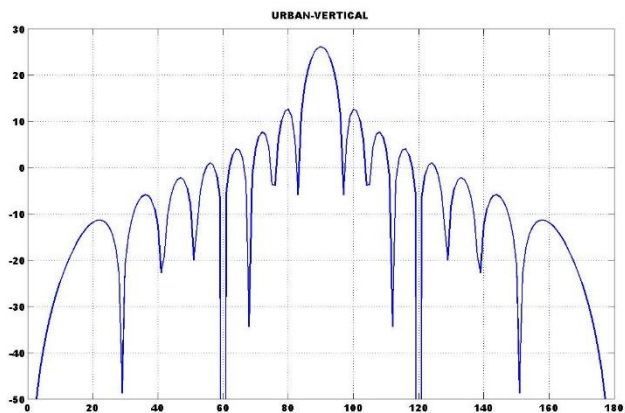


FIGURE 3-2

Horizontal plane antenna radiation patterns for urban and suburban scenarios

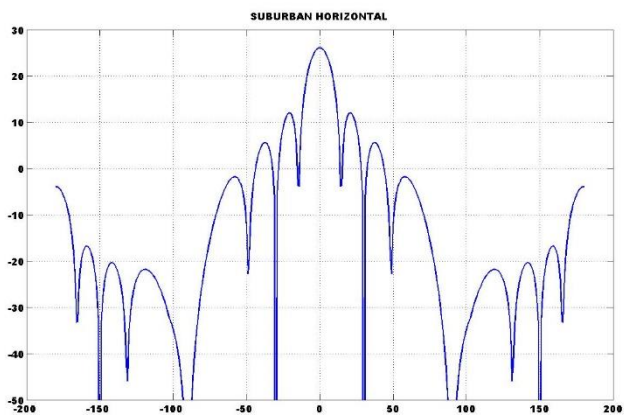
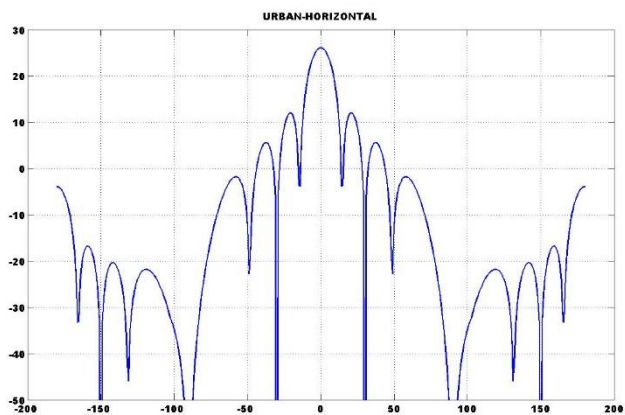
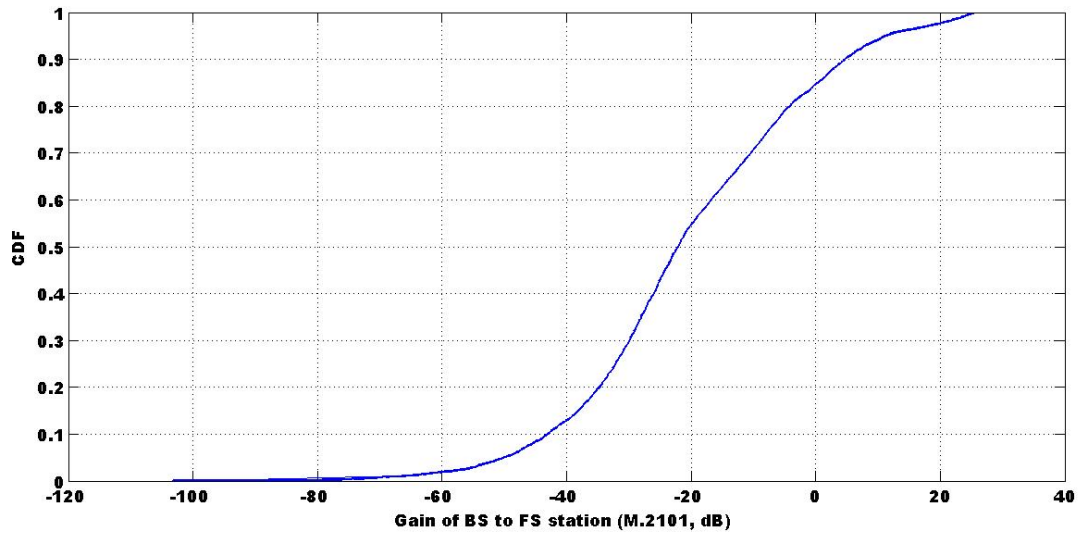


FIGURE 3-3

Antenna gain at the interfering direction in urban scenario

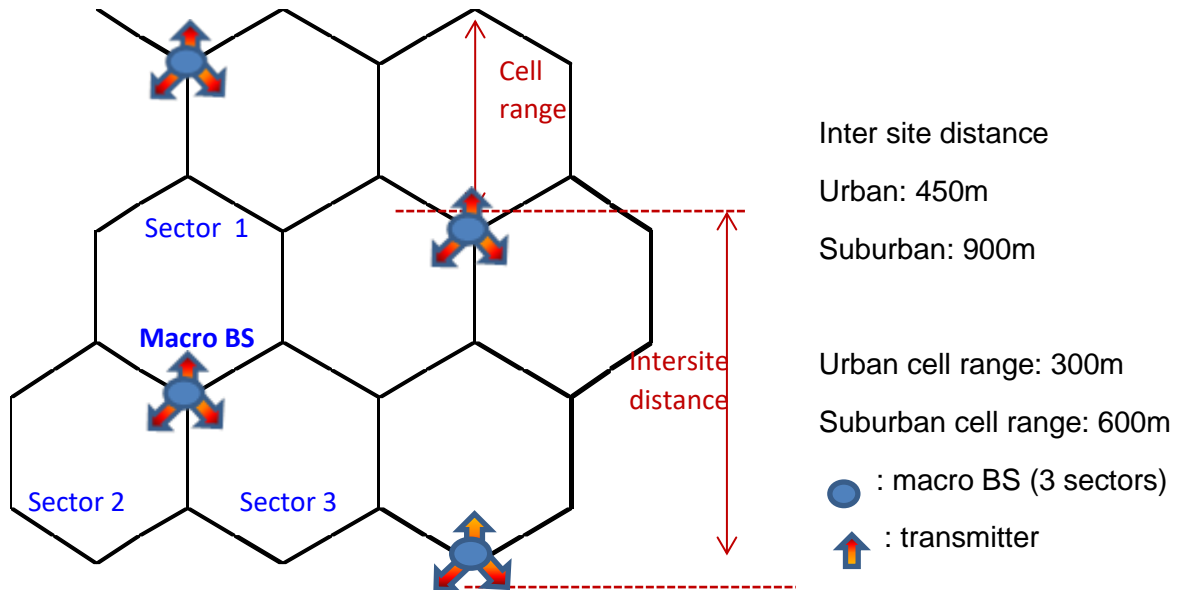


The hexagonal cell structure of the Macro BSs is recalled in the below picture.

FIGURE 3-4

Cell structure of Macro BS

IMT Base station in network (macro BS only)



---

For studies involving IMT deployments over wider areas, however, it is unrealistic to assume that IMT base stations will be deployed at the same high density across the whole area, and the deployment density values in the Table 1 need to be adjusted.

Therefore, as IMT base stations will not be deployed at the same very high density across a large area, the deployment density values will need to be adjusted for large area cases according to the ratio of coverage area to the total large area in study.

Considering the difference of propagation characteristics and available bandwidth etc., relatively large area IMT stations deployment characteristic is frequency and scenario specific, e.g. the higher frequency with larger bandwidth maybe more suitable for capacity enhancement and the deployment characteristic for large area is different from coverage. In addition, IMT station deployment in some frequency bands could be considered as complementary of existing IMT systems, e.g. base stations can be deployed in the areas where existing IMT system cannot satisfy the traffic requirement.

The deployment density values for large area ( $DI$ ) to be used in a sharing study is therefore calculated according to the following formula:

$$DI = D_s * Ra * Rb$$

where:

$D_s$  = density value for coverage area, i.e. density of simultaneously transmitting UEs or number of BS per km<sup>2</sup>; (see Table 1)

$Ra$  (%) = ratio of coverage areas to areas of cities/built areas/districts;

$Rb$  (%) = ratio of built areas to total area of region in study.

The  $Ra$  value depends on frequency band and deployment environment. The  $Ra$  for 6-8 GHz band would be larger than that for millimeter wave band, noting that 6-8 GHz band is mainly used for capacity enhancement purpose by macro cell and small cell deployments, whereas millimeter wave band is mainly used for capacity enhancement by hotspot deployment. However, IMT base stations in a particular band between 6 and 8 GHz will not be deployed across the entire area of a city, and an  $Ra$  value of 100% would greatly over-estimate the number of base stations.

$Rb$  is independent from frequency band and deployment environment. When the size of area under the study is very large assuming very large satellite-footprint or countries the  $Rb$  value needs to be decreased to reflect sparse population density of the countries.

For sharing and compatibility studies concerning potential interference into a satellite space station, it is the size of the satellite footprint that is relevant rather than countries. A large satellite footprint will in most cases cover (parts of) a number of countries (unless it is entirely within a very large country), and there may in many cases also be bodies of water within the footprint.

Considering the above, in the case of a study in the frequency band 6-8 GHz, Option 1  $Ra$  and Option 1  $Rb$  values in Table 3-4 are used in this study.

TABLE 3-4

Values for Ra and Rb to be used in studies involving IMT deployments for frequency bands between 6 and 8 GHz

	Options *	Macro	Micro
Ra	1	30% Urban (area < 200 000 km <sup>2</sup> ) 10% Urban (area > 200 000 km <sup>2</sup> ) 10% Suburban (area < 200 000 km <sup>2</sup> ) 5% Suburban (area > 200 000 km <sup>2</sup> )	10% Urban (area < 200 000 km <sup>2</sup> ) 5% Urban (area > 200 000 km <sup>2</sup> )
Rb (depending on the area under study)	1	5% (area < 200 000 km <sup>2</sup> ) 2% (200 000 - 1 000 000 km <sup>2</sup> ) 1% (area > 1 000 000 km <sup>2</sup> )	5% (area < 200 000 km <sup>2</sup> ) 2% (200 000 - 1 000 000 km <sup>2</sup> ) 1% (area > 1 000 000 km <sup>2</sup> )

---

## 4 Sharing and compatibility studies

### 4.1 Sharing and compatibility of the fixed-satellite service (FSS) (Earth-to-space) operating in the frequency band 6 425-7 025 MHz

This section presents a methodology for the evaluation of coexistence between the fixed satellite service (FSS) uplink receiver and international mobile telecommunications (IMT) system in the frequency range 6425-7125 MHz (the “6GHz band”). Urban and Suburban macro cells scenarios are considered in the study. Rural scenario is not considered because of its insignificant effect to FSS uplink service at 6GHz band. UE interference has not been included at this stage.

#### 4.1.1 Technical characteristics

##### 4.1.1.1 Technical characteristics of FSS UL system

Table 4 provides the technical and operational parameters of FSS UL systems for the frequency bands between 6 425-7 075 MHz. There are 8 carrier types provided by the document which operates in the 6GHz band and reflects a range of different FSS system designs. Carrier #1(global beam, least sensitive to interference) is considered in this study which has a high noise temperature and low peak gain. Table 4-1-1 below gives some parameters about Carrier 1 global beam.

TABLE 4-1-1  
Technical and operational characteristics of Carrier 1

Frequency range	MHz	6 425-6 725
<b>Carrier</b>	Carrier Name	1
Noise bandwidth	MHz	1
<b>Space station</b>		
Peak receive antenna gain	dBi	22
Antenna receive gain pattern and (3-dB) beamwidth	–	Recommendation ITU-R S.672- Global beam- beamwidth of 15 degrees (single, circular, oriented to sub-satellite point)
System receive noise temperature	K	630
Satellite height	km	35 840
Earth radius	km	6 378
GSO orbit	°	120° E
Coverage region size		3 dB footprint size calculated by 3 dB beamwidth parameter which covers Africa and parts of Europe and Asia



#### 4.1.1.2 Large area interference aggregation from IMT base stations

To calculate the total number of IMT base stations over the large footprints, the study examines the IMT BS cells that are located within the 3 dB beamwidth footprint of the satellite with a 15-degree beamwidth. The shape and size of the footprint on Earth can be derived from geometric considerations of the orbital position, beam size, and boresight direction of the satellite receiver.

Figure 4-1-1 below illustrates a scenario where an IMT BS cell radiates by forming a beam towards an IMT user equipment (UE) located within its coverage area. The entire network region relevant for simulations is a cluster of nineteen sites of three sectors each, where other clusters of 19 sites are repeated around this central cluster based on a wrap-around methodology employed to avoid the network deployment edge effects. The elevation angle of the signal direction is denoted as  $\theta$  (defined between  $0^\circ$  and  $180^\circ$ , with  $90^\circ$  representing perpendicular angle to the array antenna aperture). The azimuth angle is denoted as  $\varphi$  (defined between  $-180^\circ$  and  $180^\circ$ ) and  $\Psi$  is the half of satellite beamwidth of Carrier 1.

FIGURE 4-1-1 Illustrative scenario involving an IMT BS cell, an IMT UE, and a geostationary satellite

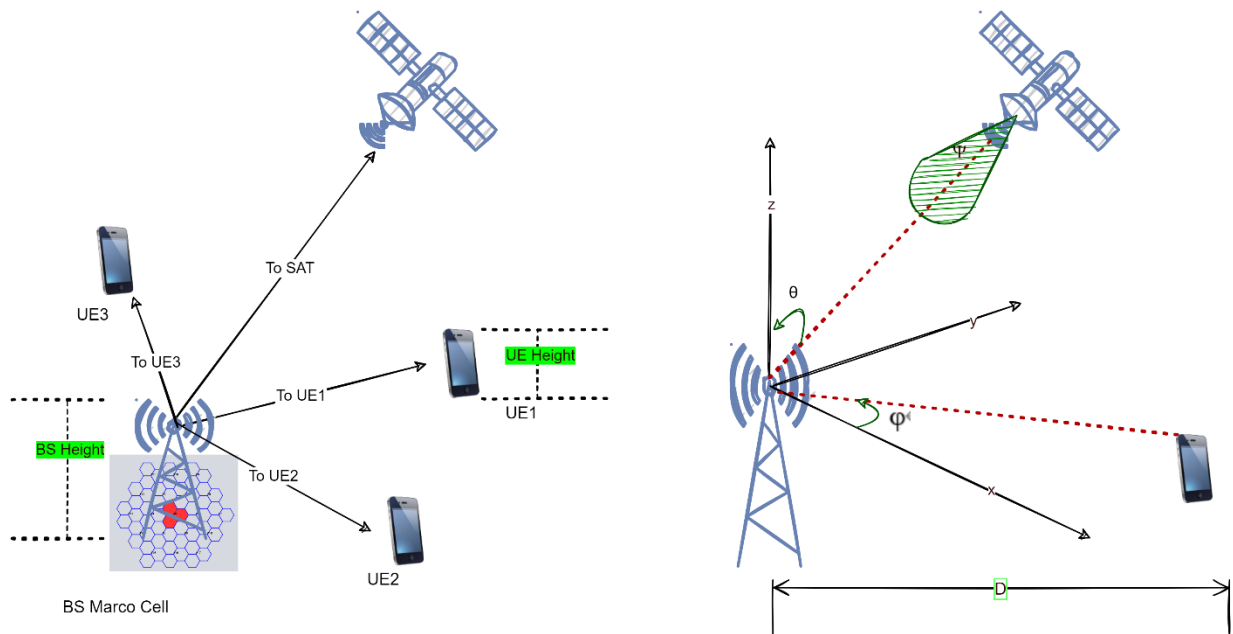
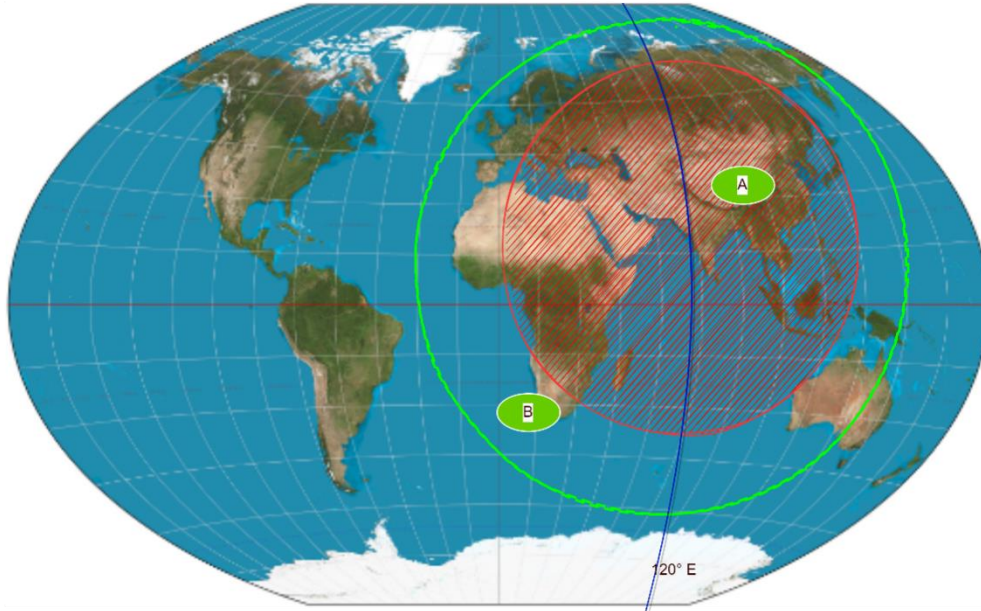


Figure 4-1-2 shows the footprint of global beam with satellite at  $120^\circ\text{E}$ . Red area A is the area of the 3 dB contour and the area of A+B covers the full visible area on the earth including some unpopulated areas, IMT base stations locate in area B are not considered in this study because of negligible interference contribution from area B. All IMT BS cells over the 3 dB footprint, but it's impossible to assume that IMT base stations are deployed at the whole area, such as deserts, oceans, virgin forests, and some other uninhabited places. Areas those are not suitable for deploying the IMT 6GHz base stations can be excluded when counting the number of base stations by using the divided pixels which shows in Figure 4-1-3.

FIGURE 4-1-2

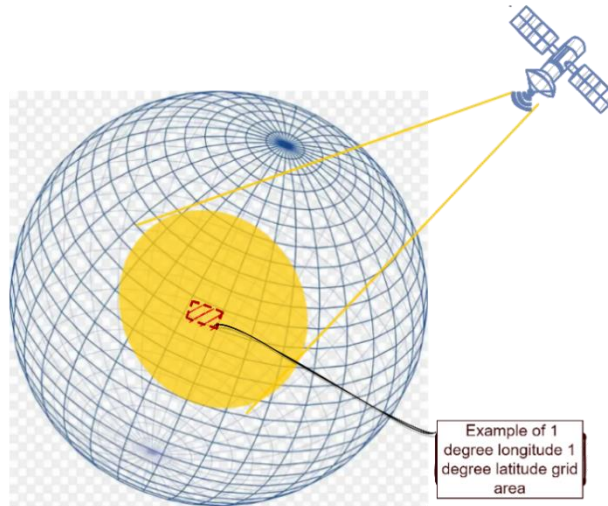
Footprint of global beam considering satellite at 120°E (3 dB contour and full visible area)



We remove parts of extremely low deployment density areas from the methodology by dividing the footprint into several pixels of  $1^\circ$  longitudes and  $1^\circ$  latitudes, then the length of an arc of  $1^\circ$  latitude is  $6378 \times \pi/180 \sim 111$  km (6378 km is the radius of the earth), and the area of a pixel is about  $111^2 \times \cos(\text{latitude})$  km<sup>2</sup>.

FIGURE 4-1-3

**Grid area of 1°\*1° longitude/latitude**



**4.1.1.3 4.1.1.3 protection criteria**

Protection criteria provides I over N (I/N) as the protection criterion, which is the ratio of the allowed inter-system interference level received in the IMT receiver relative to the receiver's noise level (thermal noise + receiver noise figure). The interference I is the total interference which can be calculated by aggregating the interference PSD. The noise N in the I/N criteria as specified above is the system receiver noise (i.e. thermal noise) and is equal to the receiver antenna noise plus the receiver noise referred to the antenna. The protection criteria values provided in Table 6 assumes the use of an I/N methodology. We use long-term protection criteria for the GSO FSS system in this study and a satellite receiver is protected if the I/N at the satellite receiver exceeds -10.5 dB with a probability that is no more than 20% which is indicated in bold in Table 4-1-2.

TABLE 4-1-2  
**Protection Criteria**

<b>Frequency Ranges</b>	<b>Percentage of time for which the I/N value could be exceeded (%)</b>	<b>I/N Criteria (dB)</b>
3 600-3 800 MHz	20%	-10.5
	0.005%	-1.3
<b>6 425-7 075 MHz (E-s)</b>	<b>20%</b>	<b>-10.5</b>
	0.001%	-2.33
	0.03%	-6

6 700-7 075 MHz (s-E)	20%	-10.5
	0.005%	-1.3

## 4.1.2 Channel model

### 4.1.2.1 Clutter Loss

“Clutter” is described here in the context of ITU-R P-series Recommendations and Clutter loss models in this Recommendation are statistical in nature. As an end correction for a long-path propagation model, “Clutter loss” is defined as the difference in the transmission loss or basic transmission loss with and without the presence of terminal clutter at either end of the path with all other path details being the same.

Specifically, it’s assumed that the probability distribution of the clutter loss is decided by the cumulative distribution function (CDF) which comes from the ITU-R WP 3K Chairman’s Report of July 2021.

“This model is applicable to urban and suburban environments. It has been developed based on measurements up to 5.7 GHz and compared against measurements between 5 and 10 GHz and ray-tracing simulations from 0.5-100 GHz, including using the method described in Report ITU-R P.2402-0. The model can be considered to be conservative with respect to the measurements between 5 and 10 GHz.”

Table 4-1-3 below is from 3K/178 which provides some input parameters for the clutter loss model.

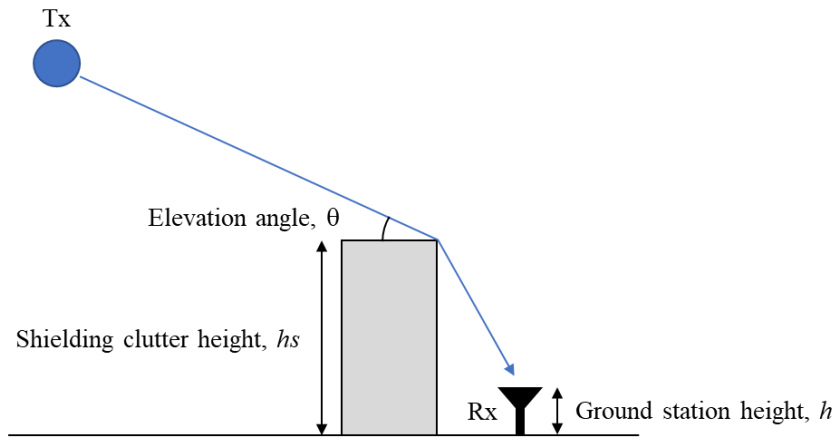
TABLE 4-1-3

#### Earth-space clutter loss model input parameters

Input	Symbol	Unit
Frequency	$f$	GHz
Elevation angle	$\theta$	Degrees
Percentage of locations	$p$	%
Shielding clutter height	$hs$	m
Ground station height	$h$	m

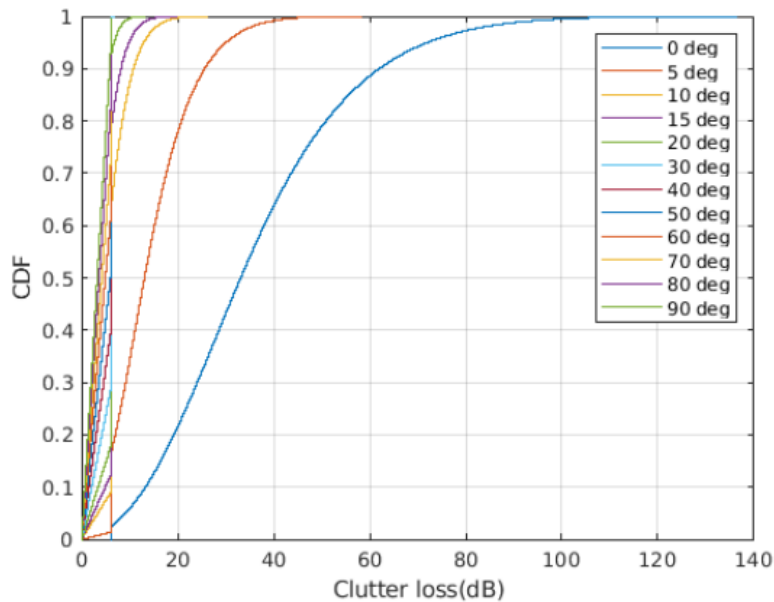
Figure 4-1-4 is the definitions of above parameters.

FIGURE 4-1-4  
Definition of parameters



We assume a frequency of  $f = 7$  GHz, a clutter shielding height of  $h_s = 25$  m, and a base station height of  $h = 18$  m in urban,  $h = 20$  m in suburban scenarios, Figure 5 shows a clutter loss CDF of  $h_s = 25$  m and  $h = 20$ :

FIGURE 4-1-5  
Clutter Loss of  $h_s = 25$  m and  $h = 20$  m



Besides the clutter loss algorithm recommended by ITU-R, we also use a method defined by the 3GPP TR 38.881.  $CL(\alpha, f_c)$  is the clutter loss defined by 3GPP and given in table 4-1-4 and table 4-1-5 at reference elevation angles for Urban and Suburban scenarios. We get aligned simulation results by using clutter loss which is defined from 3GPP and ITU-R model separately.

TABLE 4-1-4

**Shadow fading and clutter loss for urban scenario**

Elevation	S-band			Ka-band		
	LOS	NLOS		LOS	NLOS	
	$\sigma_{SF}$ (dB)	$\sigma_{SF}$ (dB)	$CL$ (dB)	$\sigma_{SF}$ (dB)	$\sigma_{SF}$ (dB)	$CL$ (dB)
10°	4	6	34.3	4	6	44.3
20°	4	6	30.9	4	6	39.9
30°	4	6	29.0	4	6	37.5
40°	4	6	27.7	4	6	35.8
50°	4	6	26.8	4	6	34.6
60°	4	6	26.2	4	6	33.8
70°	4	6	25.8	4	6	33.3
80°	4	6	25.5	4	6	33.0
90°	4	6	25.5	4	6	32.9

TABLE 4-1-5

**Shadow fading and clutter loss for suburban and rural scenarios**

Elevation	S-band			Ka-band		
	LOS	NLOS		LOS	NLOS	
	$\sigma_{SF}$ (dB)	$\sigma_{SF}$ (dB)	$CL$ (dB)	$\sigma_{SF}$ (dB)	$\sigma_{SF}$ (dB)	$CL$ (dB)
10°	1.79	8.93	19.52	1.9	10.7	29.5
20°	1.14	9.08	18.17	1.6	10.0	24.6
30°	1.14	8.78	18.42	1.9	11.2	21.9
40°	0.92	10.25	18.28	2.3	11.6	20.0
50°	1.42	10.56	18.63	2.7	11.8	18.7
60°	1.56	10.74	17.68	3.1	10.8	17.8
70°	0.85	10.17	16.50	3.0	10.8	17.2
80°	0.72	11.52	16.30	3.6	10.8	16.9
90°	0.72	11.52	16.30	0.4	10.8	16.8

**4.1.2.2 Path Loss**

Path loss describes the loss in signal strength from transmitter to receiver due to radio propagation. Free space basic transmission loss ( $L_{bfs}$ ) is the basic transmission loss assuming the complete radio path is in a vacuum with no obstruction. It depends only on the path length,  $d$  (km), and frequency,  $f$  (GHz) which is according to ITU-R P.619-4 [4]:

$$L_{bfs} = 92.45 + 20 \log_{10}(f d) \quad (\text{dB})$$

The path loss at a frequency of 7 GHz is around 200 dB at the equator, and varies by no more than ~1 dB at different locations on Earth [6]. Path loss is combined with free space basic transmission loss  $L_{bfs}$  (dB) and beam spreading loss ( $A_{bs}$ ), both described in ITU-R P.619-4.

$$L_{path}(\text{dB}) = L_{bfs}(\text{dB}) + A_{bs}(\text{dB})$$

Beam spreading loss ( $A_{bs}$ ) is specified as follows:

“Beam spreading loss, , is a non-ohmic loss due to spreading of the antenna beam in the vertical elevation plane due to the variation of the radio refractive index vs. height. This effect is insignificant for elevation angles above 5 degrees.

The signal loss due to beam spreading for a wave propagating through the total atmosphere in the Earth-space and space-Earth directions is:

$$A_{bs} = \pm 10 \log(B) \quad (\text{dB})$$

Where:

$$B = 1 - \frac{0.5411 + 0.07446\theta_0 + h(0.06272 + 0.0276\theta_0) + h^2 0.008288}{[1.728 + 0.5411\theta_0 + 0.03723\theta_0^2 + h(0.1815 + 0.06272\theta_0 + 0.0138\theta_0^2) + h^2(0.01727 + 0.008288\theta_0)]^2}$$

Where:

$\theta_0$ : elevation angle of the line connecting the transmitting and receiving points (degrees) ( $\theta_0 < 10^\circ$ )

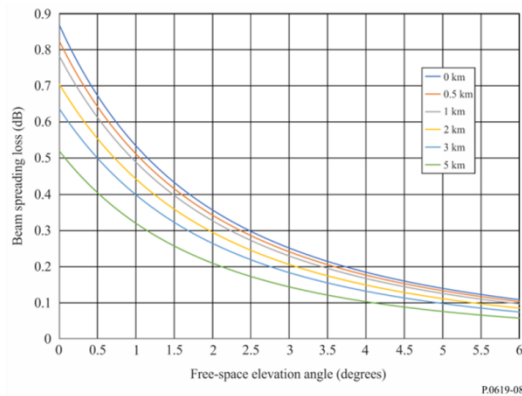
$h$ : altitude of the lower point above sea level (km) ( $h \leq 5$  km).

[...] The magnitude of the beam-spreading loss is independent of frequency over the range of 1–100 GHz.”

Figure 4-1-6 below represents beam spreading loss by the ITU-R P.619-4:

FIGURE 4-1-6

Beam spreading loss through the atmosphere in ITU-R P.619



#### 4.1.2.3 Polarisation loss

Polarization loss is indicated in the WP5D Chairman’s Report [2], it’s suggested to have a  $\pm 45^\circ$  linear polarization for the antenna elements in the arrays of an IMT base station. We set a polarization loss value of  $L_{pol} = 3$  dB [6], and this value is a common assumption in similar sharing study and is consistent with recommendations in ITU-R P.619 [4] and ECC Report 302 [5].

---

### 4.1.3 Methodology

What we have done about modelling the aggregated interference from IMT base stations to FSS satellite station receiver is based on the Recommendation ITU-R M.2101 and main steps are as the below:

Firstly, we need to calculate the total number of base stations and derive the aggregated interference caused by them. Following the approach in the WP5D Report, the number of base stations within the coverage of the satellite's 3dB bandwidth who performs downlink transmission at the same time is determined by the following formula:

$$N_{BS,u} = \sum_{k=1}^n A \times Ds \times Ra \times Rb \times LF$$
$$N_{BS,s} = \sum_{k=1}^n A \times s \times Ra \times Rb \times LF$$

Where:

$N_{BS,u}$  : total number of Urban IMT base station within the satellite footprint.

$N_{BS,s}$ : total number of Suburban IMT base station within the satellite footprint.

$\sum_{k=1}^n A$ : evaluation area size in km<sup>2</sup>,  $A$  is the area of  $k^{\text{th}}$  pixel

$Ds$ : density value for coverage area, density of simultaneously transmitting number of BS per km<sup>2</sup>, 10 BSs/km<sup>2</sup> urban and 2.4 BSs/km<sup>2</sup> suburban, defined in the table 1.

$Ra$  (%) = ratio of coverage areas to areas of cities/built areas/districts, defined in table 5.

$Rb$  (%) = ratio of built areas to total area of region in study, defined in table 5.

$LF$ : Network loading factor, described in Table 1, is equal to 0.2.

We separately calculated the number of base stations from urban and suburban scenarios due to the different deployment densities of base stations in different regions in this study.

Secondly, aggregated interference from all IMT base stations Marco cells is calculated by the following formula:

$$I_{BS,u} = F_{TDD} \sum_{n=1}^{N_{BS,u}} I_n \quad (\text{mW/MHz})$$



$$I_{BS,s} = F_{TDD} \sum_{m=1}^{N_{BS,s}} I_m \quad (\text{mW/MHz})$$

Where:

$I_{BS,u}$ : aggregated interference from urban scenario.

$I_{BS,s}$ : aggregated interference from suburban scenario.

$F_{TDD}$ : BS TDD activity factor described in Table 1.

$F_{TDD}$  represents the proportion of subframes used by the base station for downlink transmission in the actual deployment of the existing network, and the remaining part is used for the receiving process. To get the ratio of I over N (I/N), we also need to calculate the noise floor PSD, N of the satellite receiver, is given as:

$$N = k.T.B = 10^6 kT$$

Where:

$k$ : the Boltzmann's constant is equal to  $1.38 \times 10^{-23}$  W/Hz/Kelvin.

$T$ : noise temperature in Kelvins, 630 in Carrier#1.

Finally, we compare the resulting I/N with the defined long-term protection criteria. The interference margin is equal to the simulated I/N value minus the long-term protection criteria, a positive interference margin means that the interference is below satellite protection criterion; a negative interference margin means that the interference is above satellite protection criterion.

#### 4.1.4 Results

The aggregated IMT base stations interference caused by Urban macro cells and Suburban macro cells cumulative distribution function (CDF) including clutter loss defined by ITU document and 3GPP are plotted in Figure 4-1-7 and Figure 4-1-8, and 500 Monte Carlo trails are performed to get a reliable statistic of the interference by the large amount of IMT base stations.

FIGURE 4-1-7

Urban, Suburban and Combined Macro BSs aggregated interference CDF  
(Clutter Loss with ITU)

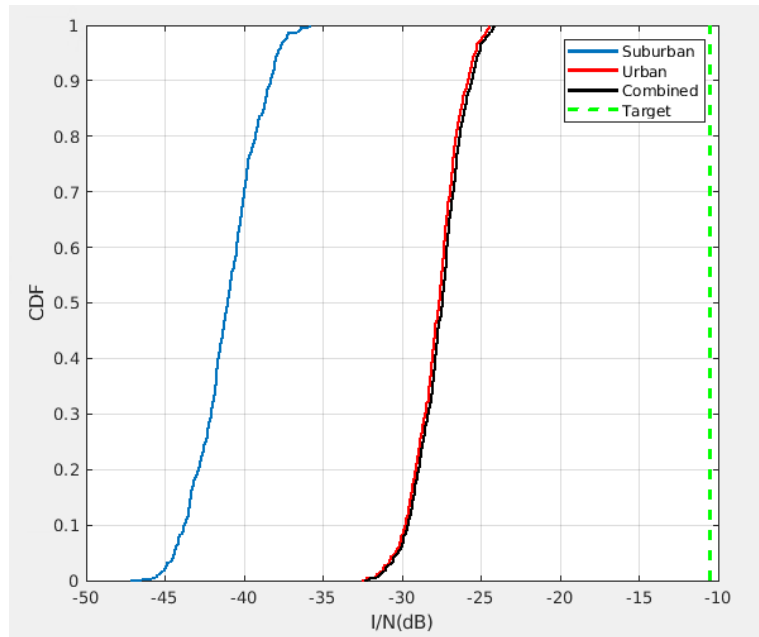
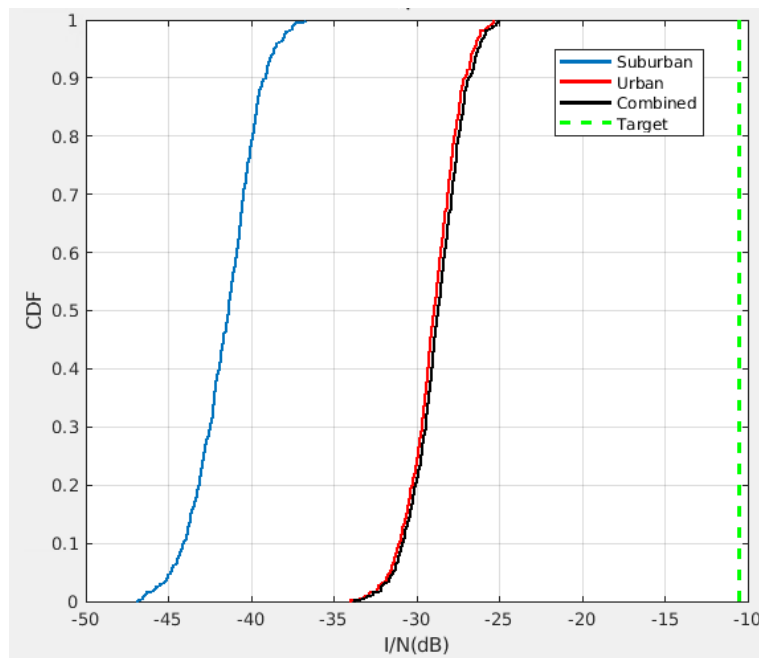


FIGURE 4-1-8

Urban, Suburban and Combined Macro BSs aggregated interference CDF  
(Clutter Loss with 3GPP)



80% CDF aggregated interference contributed by Urban Macro cells, Suburban Macro cells and combined scenario are provided in Table 4-1-6 and Table 4-1-7, which shows that different clutter loss model has little effect on the results.

TABLE 4-1-6

***I/N* comes from Urban, Suburban and Combined scenario with ITU-R clutter loss**

<b>CDF</b>	<b><i>I/N</i> interference value</b>	<b>Corresponding protection <i>I/N</i> value</b>	<b>Interference Margin (dB) compared to protection criterion</b>	
80%	-26.7	-10.5	16.2	Urban
	-39.3	-10.5	28.8	Suburban
	-26.5	-10.5	15.9	Combined

TABLE 4-1-7

***I/N* comes from Urban, Suburban and Combined scenario with 3GPP clutter loss**

<b>CDF</b>	<b><i>I/N</i> interference value</b>	<b>Corresponding protection <i>I/N</i> value</b>	<b>Interference Margin (dB) compared to protection criterion</b>	
80%	-27.7	-10.5	17.2	Urban
	-39.9	-10.5	29.4	Suburban
	-27.4	-10.5	17	Combined

#### 4.1.5 Conclusions

In this study, the interference generated by the macro base station cells to the FSS uplink satellite receiver in urban, suburban and combined scenarios for the satellite footprint examined to noise is almost 15.9~29.4 dB margin lower than the pre-defined long-term protection criteria of -10.5 dB at the range of 6 425-7 125 MHz in the considered three scenarios.

#### 4.2 Sharing and compatibility of the fixed-satellite service (FSS) (space-to-Earth) operating in the frequency band 6 700-7 075 MHz

This section comprises a coexistence study between International Mobile Telecommunications (IMT) using active antenna systems (AASs), IMT-2020, and non-geostationary (NGSO) fixed

satellite service (FSS) (space-to-Earth) including low Earth orbit (LEO) and medium Earth orbit (MEO) satellite constellations in the 6 700-7 075 MHz band. This study shows that, for urban and suburban scenarios, the FSS protection criteria are satisfied with certain separation distances. Additionally, considering a more realistic FSS ES antenna gain mask, the separation distances are reduced in around 1 to 2 km for the long-term protection criterion.

Furthermore, for the band 6 425-7 125 MHz, the study considers a sub-array implementation for the antenna model since the sub-array configurations are designed in various IMT system and performance aspects. Thus, in addition to the baseline single-element antenna configuration, in this section the study evaluates the coexistence between IMT BSs and FSS ESs considering BSs with a sub-array configuration.

Clutter model we use is random percentage of locations and only on IMT side since is expected that in urban scenarios the likelihood of higher buildings surrounding the BSs is high and for sub-urban LOS probability is very low (below 1%) for distances greater than 4.6km.

The study uses Monte Carlo simulations, to assess the aggregated interference from a deployed AAS-based IMT network towards a non-GSO FSS ES. It is considered co-channel operation of IMT-2020 and FSS deployed in the 6 700-7 075 MHz frequency range. It is also considered two real satellite constellations, Hibleo-X and Omnispace which corresponds to LEO and MEO constellations respectively.

#### 4.2.1 Technical characteristics

This section provides the IMT-2020 and FSS system and deployment related parameters used in our study.

##### 4.2.1.1 Technical and operational characteristics of FSS (space-to-Earth) operating in the frequency band 6 700 -7 075 MHz

The space-to-Earth allocation to FSS in the band 6 700-7 075 MHz is limited to feeder links for non-GSO satellite systems as specified in the footnote RR No. **5.458B** of the Radio Regulations. The FSS ES parameters considered in this study are based on the agreed technical, operational characteristics and protection criteria of FSS systems provided by WP 4A (Document [5D/734](#)). Table 4-2-1 contains the FSS ES parameters used in this study (Carrier #7 and carrier #8) and Table 4 contains the FSS protection criteria.

TABLE 4-2-1  
Downlink parameters for FSS ES

	Carrier #7 (Hibleo-X)	Carrier #8 (Omnispace)
Antenna diameter (m)	5.5	7.6
Peak antenna gain (dBi)	50	52
Antenna pattern	Rec. ITU-R S.465-6	Rec. ITU-R S.465-6
System noise temperature (K)	130	150
Antenna height (m)	5	5

	<b>Carrier #7 (Hibleo-X)</b>	<b>Carrier #8 (Omnispace)</b>
Antenna elevation angle (degrees)	Refer to non-GSO FSS Earth station elevation angle section	Refer to non-GSO FSS Earth station elevation angle section

TABLE 4-2-2  
Protection Criteria

<b>Frequency Ranges</b>	<b>Percentage of time for which the <i>I/N</i> value could be exceeded (%)</b>	<b><i>I/N</i> Criteria (dB)</b>
6 700-7 075 MHz (s-E)	20% 0.005%	-10.5 -1.3

The protection criteria specified are related to the required availability of FSS links which is associated with time. However, Monte Carlo sharing studies conducted between FSS and IMT-2020 systems under WRC-23 agenda item 1.2 may involve other considerations based on additional variables which are not varying in the time domain (e.g. geographical locations in the space or deployment domain associated with IMT positions). Thus, it may be appropriate to understand percentages as being in other domains, such as time, location, and probability.

Additionally, although no more specifications of the FSS ES receiver have been established, it is important to account for the following aspects of the FSS ES: the antenna efficiency is below 100%, the actual gain of the sidelobes is below the values in Rec. ITU-R S.465-6, among others. Thus, we include a sensitivity analysis using a more realistic FSS ES antenna gain mask as indicated in the [5D/1140](#) which considers the preceding aspects.

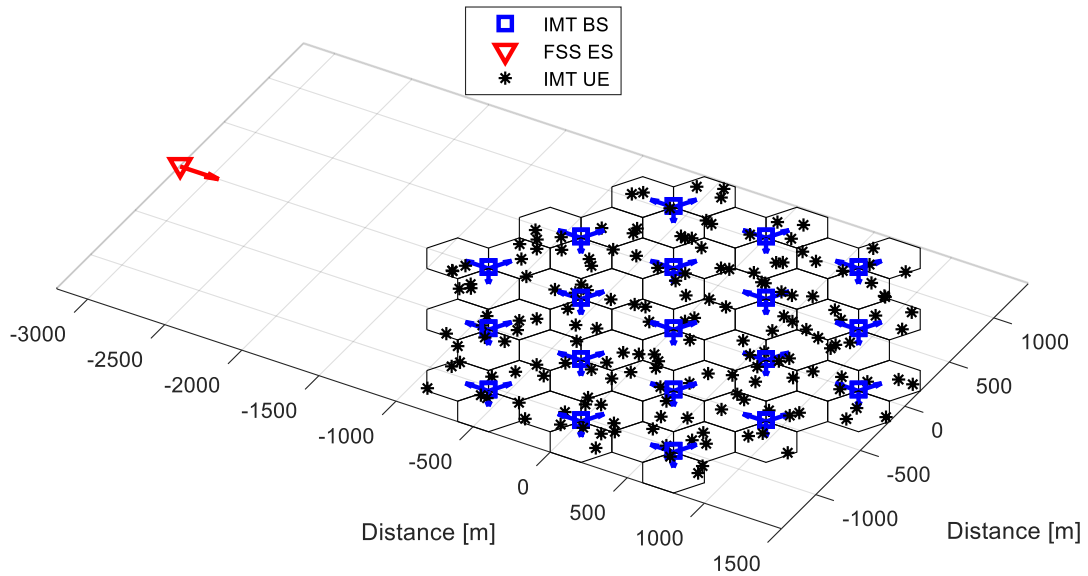
#### 4.2.2 Methodology

Based on the questionnaire about the use of the 6 425-7 075 MHz band in Europe ([ECC PT1\(21\)067](#)), an FSS ES located in the south of France (44° N, 2° E) is assumed to perform this study. This FSS ES is a gateway station which is located in a rural area and operates as a downlink non-GSO feeder link.

The IMT-2020 network consists of a 19-sites cluster where each site comprises 3 hexagonal sectors leading to 57 BSs in total. In each snapshot of the Monte Carlo simulation, 3 UEs with random azimuth angles are randomly located within each sector where both azimuth and location are uniformly distributed. The FSS ES antenna azimuth is assumed to be in the direction of the center of the 19 sites cluster. Figure 4-2-1 shows an exemplary deployment snapshot with a separation distance between the FSS ES and the closest BS of 2 km.

FIGURE 4-2-1

Deployment comprising a single FSS ES and a IMT 19-sites cluster



To determine the FSS ES elevation angle range and distribution, real non-GSO satellite constellations are considered and it is assumed that the FSS ES is continuously tracking the closest satellite. Table 4-2-3 contains the parameters of the satellite constellations used in this study.

TABLE 4-2-3

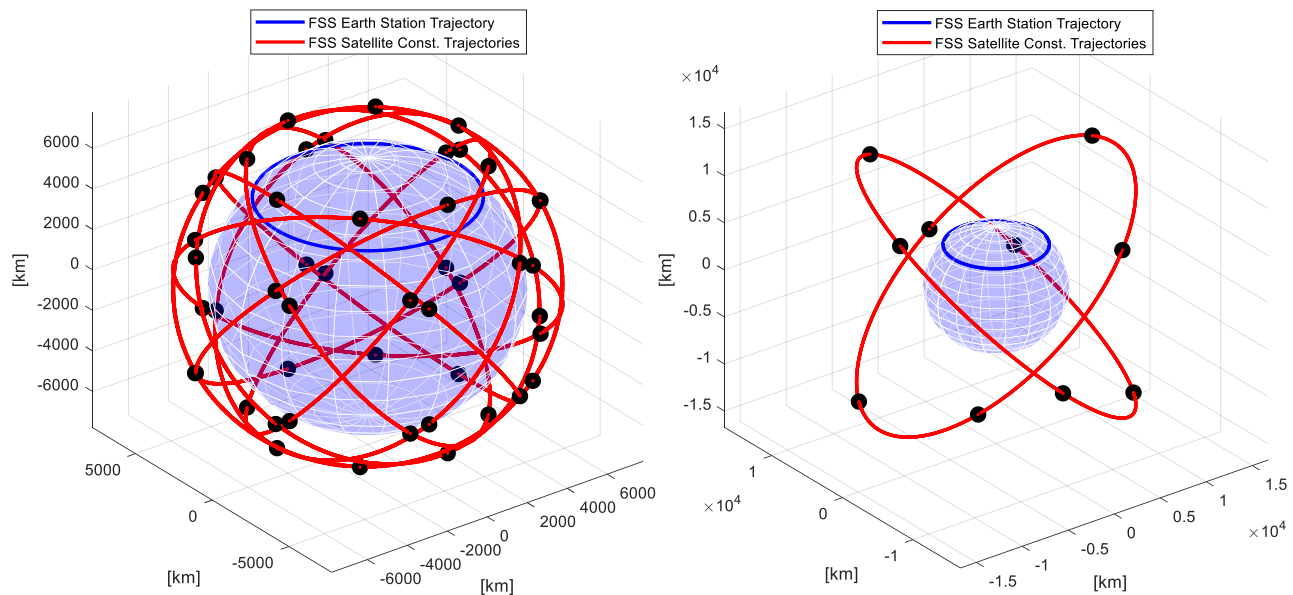
non-GSO satellite constellations parameters

	Carrier #7 (Hibleo-X)	Carrier #8 (Omnispace)
Type of constellation	LEO	MEO
Orbit radius (incl. Earth's radius) (km)	8145	17091
Orbit period (s)	6840	21540
Satellite angular velocity (deg/s)	0.0526	0.0167
Orbit inclination (degrees)	52	45
Number of satellites per orbit	6	5
Right ascension of the ascending node (RAAN) of all orbits (degrees)	0, 45, 90, 135, 180, 225, 270, and 315	63.64 and 243.64

Figure 4-2-2 shows the FSS satellites trajectories and the FSS ES trajectory located in the latitude 44° N.

FIGURE 4-2-2

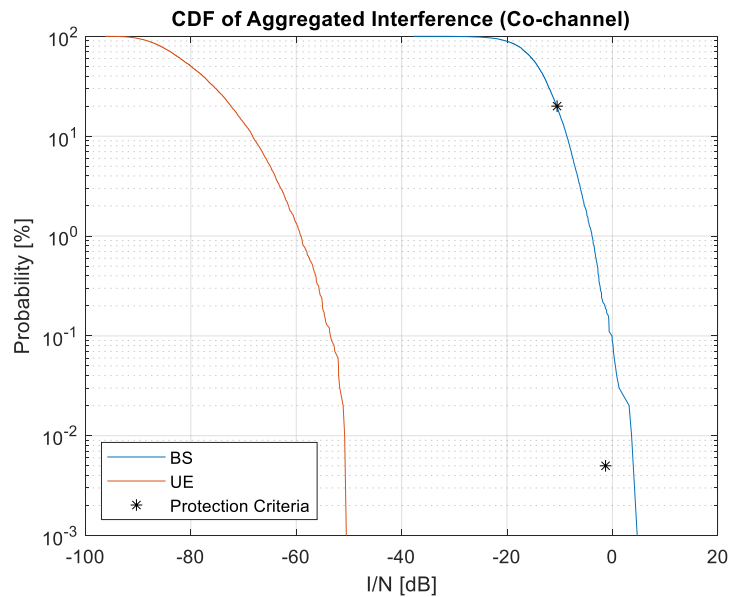
FSS ES and satellites trajectories. Hibleo-X (left) and Omnispace (right)



### 4.2.3 Study Results

For a separation distance of 16 km between the Hibleo-X FSS ES and the closest BS, Figure 4-2-3 shows the CDF curves of the aggregated  $I/N$  from the BSs and the UEs. As can be seen, the long-term protection criterion is not exceeded by any of the curves.

FIGURE 4-2-3  
CDF curves of the aggregated  $I/N$  from BSs and UEs for Hibleo-X FSS ES



It is noted that the percentages of the aggregated  $I/N$  CDFs curves presented in our study correspond to percentage of snapshots.

#### 4.2.3.1 Results with AASs with and without sub-arrays

In addition to the single-element beamforming antenna characteristics in Table 4-2-4, in Table 6 are provided the parameters for an antenna array using sub-arrays for this band. It should be noted that the total conducted power is the same and only the size and array configuration is changed.

Antennas with sub-arrays are typically used to optimize the antenna design by providing a certain aperture size while reducing the number of radios required. Sub-arrays are typically used to optimize the antenna design, especially in the vertical domain as users are located within a typical steering range for the specific scenario. Since multiple antenna elements are combined together to form a "logical" element, i.e., a sub-array, the radiation pattern of the "logical" element becomes narrower in the vertical plane as compared to the single-element case. This can additionally help in reducing the side lobe gain levels. Furthermore, sub-arrays are designed with an electrical down tilt so that the sub array beam is focused towards the intended terrestrial users. Thus, while



---

grating lobes may occur due to the sparse arrays (sub-array spacing  $> 0.5 \lambda$ ) depending on the steering angle, the downtilt can mitigate the impact of these grating lobes.

TABLE 4-2-4

**Antenna and power characteristics for IMT-2020 BSs with sub-arrays**

	<b>Urban Macro / Suburban</b>
Antenna pattern	Refer to the extended AAS model in WP 5D <a href="#">Chairman's Report Annex 4.4</a> (Table A of Annex 3)
Element gain (incl. Ohmic loss) (dBi) <b>(Note 1)</b>	6.4
Horizontal/vertical 3 dB beamwidth of single element (degree)	90° for H 65° for V
Horizontal/vertical front-to-back ratio (dB)	30 for both H/V
Antenna polarization	Linear $\pm 45^\circ$
Antenna sub-array configuration (Row x Column) <b>(Note 2)</b>	16 x 16
Horizontal/Vertical radiating sub-array spacing	0.5 of wavelength for H 1.4 of wavelength for V
Number of element rows in sub-array	2
Vertical radiating element spacing in sub-array	0.7 of wavelength
Pre-set sub-array downtilt (degrees)	3
Array Ohmic loss (dB) <b>(Note 1)</b>	2
Conducted power (before Ohmic loss) per sub-array (dBm) <b>(Notes 5, 6)</b>	19
Base station maximum coverage angle in the horizontal plane (degrees)	$\pm 60$
Base station vertical coverage range (degrees) <b>(Notes 3, 4, 7)</b>	90-100
Mechanical downtilt (degrees) <b>(Note 4)</b>	6 / 3

**Note 1:** The element gain includes the array Ohmic loss and is per polarization. This means that the array Ohmic loss is not needed for the calculation of the BS composite antenna gain and e.i.r.p.

**Note 2:** For the extended AAS model case, 16 x 16 means there are 16 vertical and 16 horizontal radiating sub-arrays.

**Note 3:** The vertical coverage range is given in global coordinate system, i.e. 90° being at the horizon.

**Note 4:** The vertical coverage range includes the mechanical downtilt.

**Note 5:** The conducted power per element assumes 16 x 16 x 2 sub-arrays for the macro case (i.e. power per H/V polarized element).

**Note 6:** In sharing studies, the transmit power calculated using the conducted power is applied to the typical channel bandwidth given in Table 7-1 and 8-1 respectively for the corresponding frequency bands of 5D/716 Chapter 4 Annex 4.4.

**Note 7:** In sharing studies, the UEs that are below the base station vertical coverage range can be considered to be served by the "lower" bound of the electrical beam, i.e., beam steered towards the max.

**Urban Macro / Suburban**

coverage angle. A minimum BS-UE distance along the ground of 35 m should be used for macro environments.

To perform simulations with the proposed antenna model with sub-arrays, the same considerations and methodology discussed in the previous sections are used.

Furthermore, additional simulations were carried out where clutter losses are applied to both the IMT BSs and the FSS ES in urban scenarios. It is noted that it's important to consider results where clutter loss is applied on the FSS side, thus, argumentation can be provided to justify implementing of additional mitigation schemes, e.g., shielding.

Table 4-2-5 presents the summary results for both the IMT BS antenna model with and without sub-arrays.

TABLE 4-2-5  
Summary results: Long-term criterion

Scenario	Clutter Loss	NGSO Satellite Constellation	Antenna Model	Separation distance
Urban	Only IMT side	Hibleo-X	Single-element	16 km
			Sub-array	7 km
		OmniSpace	Single-element	15 km
			Sub-array	6 km
	IMT and FSS ES side	Hibleo-X	Single-element	< 1 km
			Sub-array	< 1 km
		OmniSpace	Single-element	< 1 km
			Sub-array	< 1 km
Suburban	Only IMT side	Hibleo-X	Single-element	18 km
			Sub-array	15 km
		OmniSpace	Single-element	17 km
			Sub-array	13 km

**4.2.3.2 4.2.3.2 Sensitivity analysis (realistic FSS ES antenna gain)**

We provide additional results using a more realistic FSS ES antenna gain mask as indicated in the 5D/1140. Figure 13 shows the comparison between the FSS ES antenna gain mask defined in Rec. ITU-R S.465 and the proposed mask in 5D/1140 assuming a peak gain of 50 dBi.

FIGURE 4-2-4

Comparison between the FSS ES antenna gain mask in Rec. ITU-R S.465 and 5D/1140

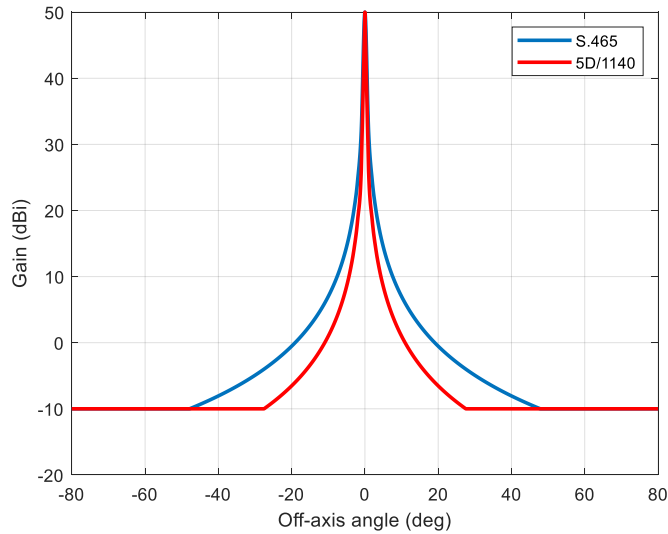


Table 4-2-6 contains the summary results for Hibleo-X constellation.

TABLE 4-2-6

Summary sensitivity analysis results: Long-term criterion (realistic FSS ES antenna gain)

Scenario	Clutter Loss	NGSO Satellite Constellation	Antenna Model	Separation distance
Urban	Only IMT side	Hibleo-X	Single-element	14.7 km
			Sub-array	5 km
Suburban	Only IMT side	Hibleo-X	Single-element	16.8 km
			Sub-array	13.6 km

From the preceding results, it is noted that the required separation distances are reduced in about 1 to 2 km when using a more realistic FSS ES antenna gain mask as the one proposed in 5D/1140.

#### 4.2.4 Summary and analysis of the results

This section provides simulation results of coexistence studies between IMT-2020 using AASs and non-GSO FSS (space-to-Earth) including LEO and MEO satellite constellations in the 6 700-7 075 MHz band. The study results show that the aggregated interference in urban macro and suburban scenarios from IMT BSs to a FSS ES is able to satisfy the FSS long-term protection criterion for all the evaluates cases at a separation distance up to 18 km for a LEO FSS ES and at a separation distance up to 17 km for a MEO FSS ES. Additional results show that, if the FSS ES has natural and/or artificial shielding in urban scenarios, the required separation distances are below 1 km.

Furthermore, from the results with the proposed antenna model with sub-arrays, it is noted that the required separation distances are reduced in about ~3-9 km due to the increased effective

aperture and directivity of the IMT BSs antenna arrays. It is noted that anticipated IMT-2020 deployments in the 6 GHz band will focus on high-capacity coverage across urban areas reusing existing 3.5 GHz band deployments infrastructure. Thus, 6 GHz band IMT-2020 deployments will not be expected in rural areas facilitating the coordination between IMT-2020 and non-GSO FSS ES in non-urban areas.

### 4.3 Sharing and compatibility of the fixed service and IMT

#### 4.3.1 Technical characteristics

##### 4.3.1.1 Technical and operational characteristics of FS operating in the frequency band 6 425-7 125 MHz

The fixed service parameters were configured according to Document 5D/583 and summarized in Table 4. The antenna heights of the transmitter and receiver were 20 and 60 meters. The modulation order of 64-QAM and channel bandwidth of 40 MHz were considered. The antenna pattern used was the Recommendation ITU-R F.1245. The link length depending on the type of FS station was varying from 10 to 38 km. In simulations different deployment of FS receivers was considered, the victim FS receiver was placed with both main lobe and side lobe pointed to the IMT-2020 network.

TABLE 4-3-1  
Simulation parameters of fixed service

System parameters	Rural area		Urban area	
Modulation	64-QAM		64-QAM	
	Example 1	Example 2	Example 3	Example 4
Channel spacing and receiver noise bandwidth (MHz)	40	40	40	40
TX output power (dBW)	3	3	3	3
Feeder/multiplexer loss (dB)	1.8	1.8	1	1.8
Antenna gain (dBi)	38	39.5	36	38
Receiver noise figure (dB)	5	5	5	5
Antenna height(m)	60	60	20	60
Link length (km)	38	38	10	35
Antenna pattern	Recommendation ITU-R F.1245			

Note 1: There is no limitation regarding FS deployment in each type of areas. Links with the receiver end in rural and the transmitter end in urban can be treated as a rural case, in order to better protect the FS.

Note 2: There are FS deployments with a range of values wider than those indicated in the table.

#### Interference criteria

Protection criteria interference to receiver thermal noise of FS service are given in Recommendation [ITU-R F.758-7](#). The interference criterion is:

---

$$I/N \leq -10 \text{ dB}$$

where:

$I$ : The interference power for FS, dBm;

$N$ : Receiver noise, dBm.

This is the long-term (no more than 20% of the time) interference protection criterion for the FS in the frequency bands of above 3 GHz.

Further, there are some regional protection criteria for actual operation reference. The operation protection criterion can be defined as below.

$$C/I \geq 30 \text{ dB}$$

where:

$C$ : The carrier power received by FS station, dBm;

$I$ : The interference power for FS station, dBm;

#### **4.3.1.2 2.4.1.3 Propagation models for sharing and compatibility studies for IMT operating in 6 425-7 125 MHz**

There are some ongoing discussions about the parameters of propagation models.

**1<sup>st</sup> is about the adoption and location percentage of clutter loss in suburban area.** The average clutter height of suburban in ITU-R P.452 is 9m which is an old data from the statistics of year 1997 or earlier. The suburban clutter can be pretty high now, but there is no representative contemporary data. In this study, clutter loss are applied to 100% IMT Base Stations with location variability p% random range from 0 to 100%.

**2<sup>nd</sup> is about the adoption of clutter loss for FS receiver.** The FS main lobe should always be assumed above clutter, due to the method of operation of a FS link. This study applies clutter loss to FS 20m height receiver with location variability p% random range from 0 to 100%.

**3<sup>rd</sup> discussion is whether the clutter loss should be correlated with the above/below rooftop ration.** The relationship between these two parameters cannot be confirmed now. In this study, clutter losses are applied to 100% IMT Base Stations with location variability p% random range from 0 to 100%.

**4<sup>th</sup> is about the selection of time percentage of propagation model.**

Generally, the Monte Carlos snapshot may not be time driven, so it can not directly match the time percentage. However, in order to reflect the time percentage in protection criteria, snapshots can be used to approximate the time slot, and then a certain probability value is taken on the I/N CDF curve to represent the time percentage in the protection criterion. The premise of this approach is that the number of snapshots is sufficient (to ensure that the simulation results can converge) and the values are random. Based on that, in this simulation, the time percentage in protection criterion has been reflected by I/N CDF.

The propagation loss is not independent from other variables (such as percentage of location, BS beam pointing). If the time percentage in protection criterion (e.g. 20%) is considered in the propagation model and also CDF curve (e.g. 80%), the real percentage may not be the time

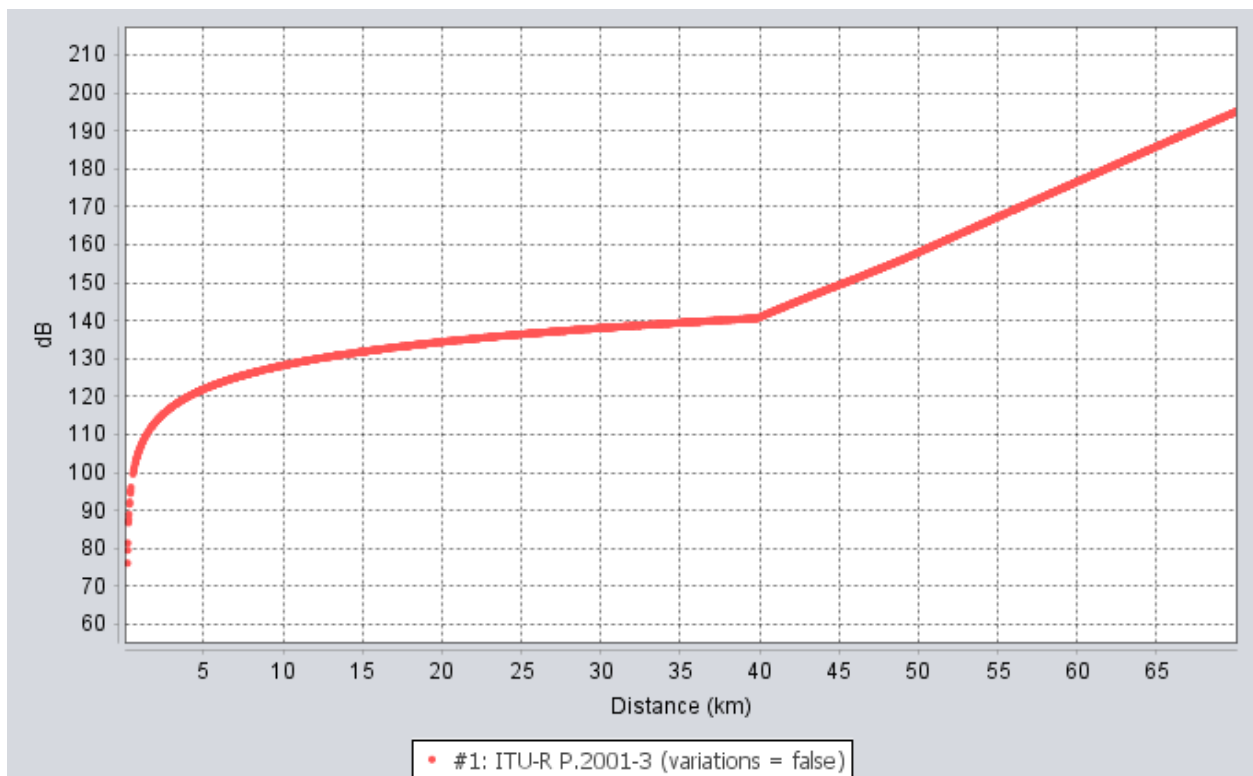
percentage in protection criterion (e.g. 20%), and it may overestimate the interference. Therefore, it is relatively fair to select a median 50% time percentage for the propagation model, and the final time percentage in protection criteria is reflected by the value of CDF.

The propagation model between IMT system and FS is from Recommendation [ITU-R P.2001-3](#). The values of parameter  $p=50\%$  is used (time percentage for which the calculated basic transmission loss is not exceeded).

Figure 5 presents pathloss curves for Recommendation ITU-R P.2001 with 50% percentage. Frequency is 6 725 MHz, transmitter height is 18m and receiver height is 60m.

FIGURE 4-3-1

Pathloss curves for Recommendation ITU-R P.2001 with 50% percentage



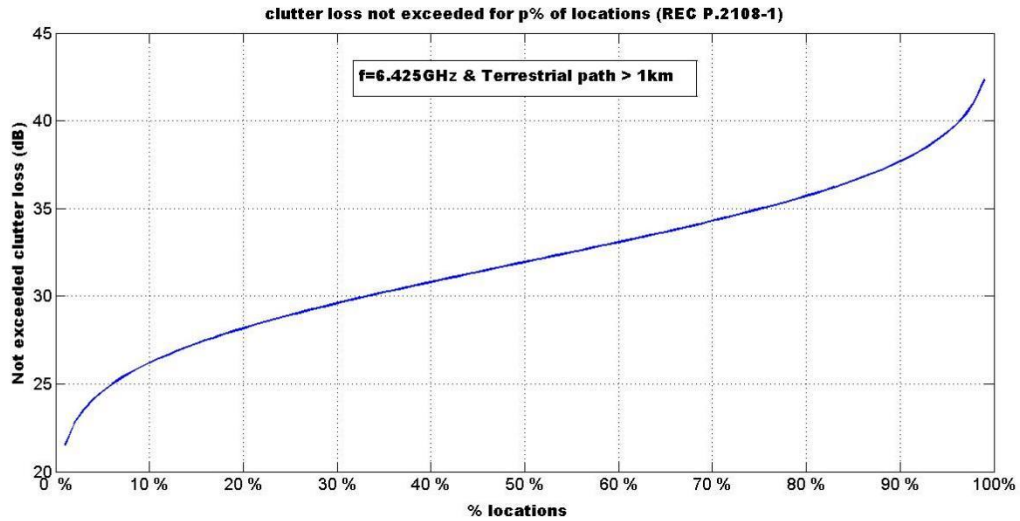
### Clutter model

The clutter loss model used in this report is defined in section 3.2 of the Recommendation ITU-R P.2108 by a statistical model for end correction of terrestrial to terrestrial long-path propagation.

Figure 4-3-2 plots the clutter distribution function for frequency 6.725 GHz and propagation paths longer than 2 kilometres. This clutter model indicates that 5% of base station locations not exceed 25 dB loss, 50% of locations with loss below 32 dB, and 95% of locations with loss below 39 dB.

FIGURE 4-3-2

**Clutter loss distribution for terrestrial paths**



The FS-FS Los path/communication does not exclude the possibility of FS receiver - IMT transmitter NLOS interference path. So that, clutters are applied to urban FS station (height≤20m) no matter IMT BS is located in suburban or urban scenario. The average clutter height depends on the surroundings. There is no parameters like “above/below clutter ratio”, so random clutter loss (uniform 1~99%) is used in this simulation with a minimum clutter of 21.5 dB for 1% of locations and a maximum of 42.4 dB for 99% of locations.

**4.3.2 Methodology**

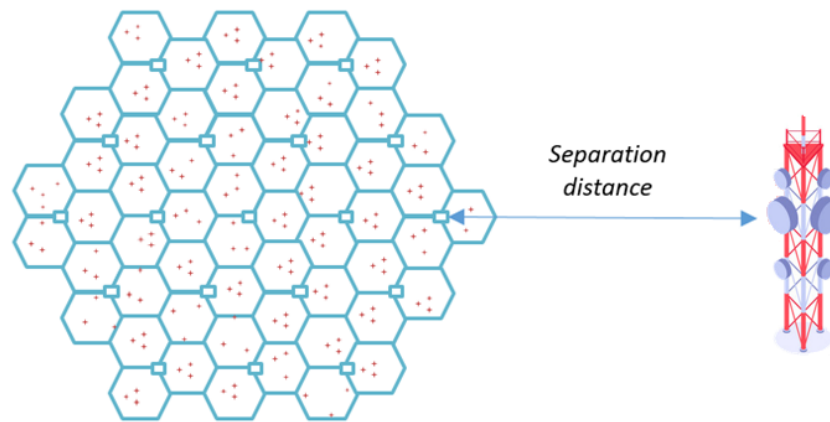
Monte-Carlo simulations are performed over the IMT mobile network and the FS station within the area of simulation to calculate the aggregated interference caused by the BSs/UEs in order to derive a reliable statistic taking into account many parameters variations (i.e. deployment characteristics, clutter variation, etc.).

The methodology of modelling IMT BSs/UEs interference into FS station receiver used in this study follows guidance of Recommendation ITU-R M.2101.

In this study, all active IMT base stations are generated in hexagon grid with 19 sites with 3 sectors. FS station is generated far away from IMT network based on the separation distance. Separation distance is measured between FS station and the edge of IMT network. In order to evaluate the worst case, FS station horizontal boresight always point to IMT networks, which means that horizontal off-axis angle of FS station is always 0 degree.



FIGURE 4-3-3  
**Simulation topology**



UE is uniformly deployed in BSs serving region based on cell radius and other parameters provided in previous table. BSs AAS beamforming direction is pointing to the location of its serving UEs.

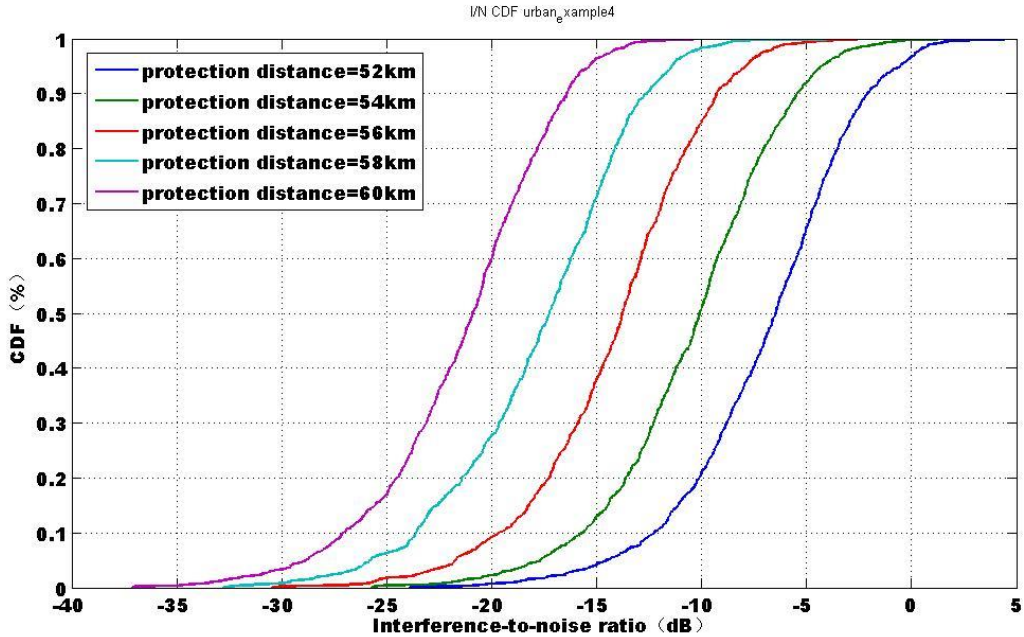
### 4.3.3 Study results

#### 4.3.3.1 Result based on I/N criterion

The implications of aggregate interference have been analysed by assuming that the FS station (example 4) receiver is at 52-60 km from the IMT cluster(urban), it can be found that total 80% aggregate interference at the FS station receiver is less than  $-119$  dBm/MHz as if protection distance is more than 56 km as shown below.

FIGURE 4-3-4

I/N Probability at 52-60 km from IMT cluster for Aggregate Interference into FS station example 4



The analysis repeated for all FS station and results are summarized below.

TABLE 4-3-2

Separation distances between IMT-2020 and FS based on $I/N \leq -10$ dB long term protection criteria	FS station #1	FS station #2	FS station #3	FS station #4
	without clutter	without clutter	with random clutter	without clutter
<b>Main lobe</b>				
Suburban (with random clutter) (km)	57	58	25	57
Urban (with random clutter) (km)	55	56	24	55
<b>Side lobe (50°)</b>				
Suburban (with random clutter) (km)	4	4	2.5	4
Urban (with random clutter) (km)	2	2	1.5	2

The in-band sharing studies between the FS and IMT showed that separation distances of the FS receivers from the edge of the IMT-2020 networks should be from 24 to 57 km depending on the FS station antenna height and IMT-2020 deployment scenario for the main lobe interference scenario and from 1.5 to 4 km depending on the FS antenna height and IMT-2020 deployment scenario for the side lobe interference scenario.

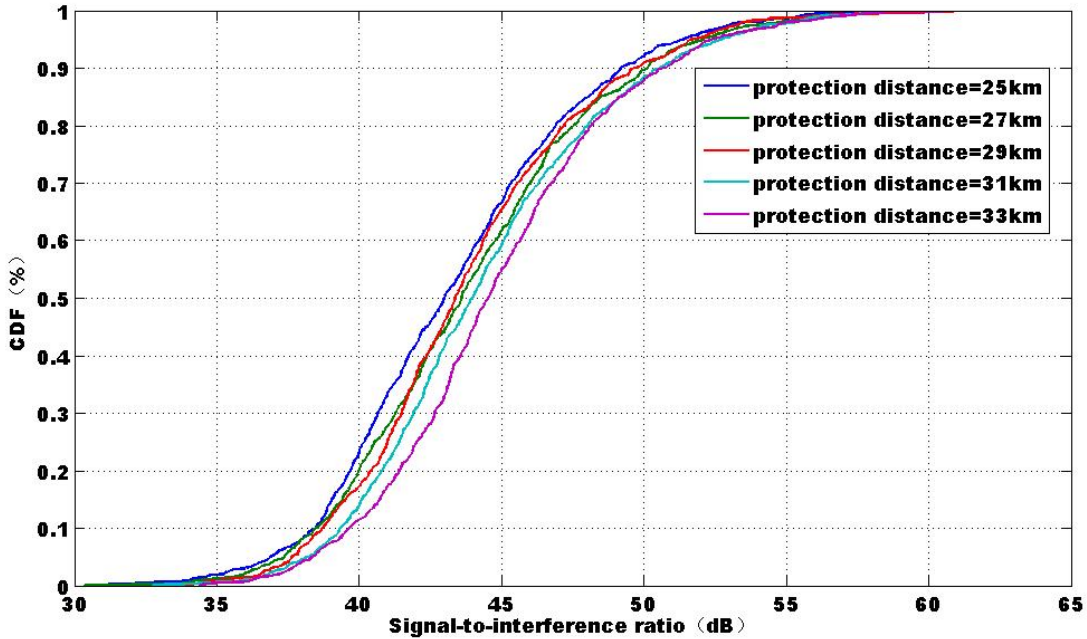
**4.3.3.2 2.4.3.2 Result based on C/I criterion**

The implications of aggregate interference have been analyzed by assuming that the FS station (example 4) receiver is at 25-33 km from the IMT cluster(urban), it can be found that total 100%

aggregate interference at the FS station receiver is less than  $-83.85$  dBm/MHz (equal to  $C/I \geq 33$ ) as if protection distance is more than 29 km as shown below.

FIGURE 4-3-5

C/I Probability at 25-33 km from IMT cluster for Aggregate Interference into FS station example 4



The analysis repeated for all FS station and results are summarized below.

TABLE 4-3-3

Separation distances between IMT-2020 and FS based on $C/I \geq 33$ dB	FS station #1	FS station #2	FS station #3	FS station #4
	without clutter	without clutter	with random clutter	without clutter
<b>Main lobe</b>				
Suburban (with random clutter) (km)	31	31	3	31
Urban (with random clutter) (km)	29	31	2	29
<b>Side lobe (50°)</b>				
Suburban (with random clutter) (km)	<1	<1	<1	<1
Urban (with random clutter) (km)	<1	<1	<1	<1

The in-band sharing studies between the FS and IMT showed that separation distances of the FS receivers from the edge of the IMT-2020 networks should be from 2 to 31 km depending on

---

the FS station antenna height and IMT-2020 deployment scenario for the main lobe interference scenario and less than 1km for the side lobe interference scenario.

#### **4.3.4 Summary and analysis of the results**

Considering wanted signal the protection criteria of the FS receivers will be  $C/I \geq 30$  dB and in that case, protection distances will be from 2 to 31 km for the main lobe scenario and less than 1 km for the side lobe scenario.

Studies found that the separation distance is necessary for the coexistence between two systems.

- For the FS antenna main lobe interference scenario, the sensitivity analysis using a C/I criterion found that the separation distances will be from 1.5 in urban scenario and 31 km in suburban for the main lobe scenario and less than 1.5 km for the side lobe scenario.

The studies summarized above showed that coexistence between IMT and the fixed service can be achieved but would require site by site coordination if IMT and FS are deployed in the same or in adjacent geographical areas.

#### **4.4 Sharing and compatibility of the SRS operating in the frequency band 7 145-7 190 MHz**

This study considers interference from a globally deployed IMT system to a victim receiver that is very far away in deep space. In particular, we consider IMT deployed in the 6 425-7 125 MHz frequency range and the space research service (SRS (deep space)) in the 7 145-7 190 MHz band. The SRS service under consideration may have stations orbiting various planetary bodies. In this initial study we concentrate on the Mars Express orbiter.

Mars Express is around 54 million km distant at Mars' closest approach to Earth and can see very nearly half the surface of the Earth at any instant. Over the course of one day Mars will appear to rise and set as seen from the Earth. At any instant there will be base stations somewhere on Earth that see the victim at low elevation, higher elevation and all elevation angles in between. Hence, a range of interference levels are incident to the satellite receiver due to variations in the interference geometries involved.

Because of the large scale of the IMT deployment, we model and deploy equivalent objects that are representative of many IMT base stations. The study models interference sourced from an IMT network deployed on the surface of the Earth incident to the distant Mars Express space station receiver in Visualyse Interplanetary software. The method used in this initial study addresses the variable and uncertain nature of this interference scenario whilst remaining relatively conservative and tractable.

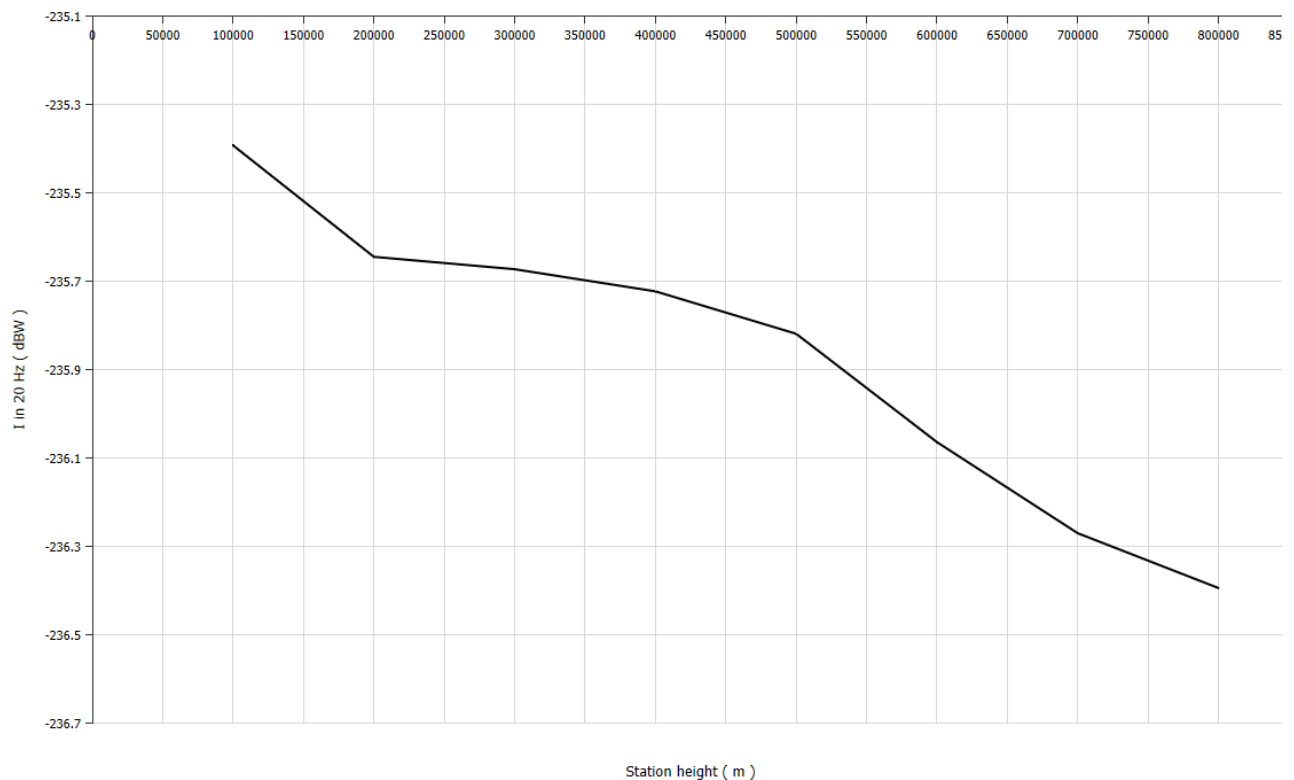
This study considers interference from IMT network deployment over the land surface of the Earth to a victim SRS satellite receiver that is in early/return mission phase/orbit around the Earth. In particular, the study considers IMT deployed in the 6 425-7 125 MHz frequency range and the space research service (SRS) (Earth-to-space) in the 7 145-7 190 MHz band.

The SRS service under consideration may be on a station in LEO orbit and/or in Launch and Early Orbit Phase (LEOP) or in the mission return phase. Each mission will have unique orbital parameters and widely varying orbital characteristics.

For reasons discussed below, a critical parameter in the determination of the instantaneous interference level is the orbit height. It can be seen below that all results are for an orbit altitude of 200 km.

Changes in altitude have two compensating effects – path loss increases proportional to the square of the distance and the area visible to the SRS space station increases proportional to the square of the distance, and the two effects produce opposite effects on the overall interference level. The combined impact of varying the orbit height is shown in the figure below. Results were calculated for different orbit heights for comparative purposes (with slightly different modelling set-up than in current version of this study), as shown in Figure 4-4-1, in order to verify that 200 km is the worst case altitude. We see a variation of around 1 dB between 200 km and 800 km orbit height, with the higher interference levels at the lower altitudes.

FIGURE 4-4-1  
Variation of Aggregate I with Orbital Altitude



At any instant there will be base stations somewhere on Earth that see the victim at low elevation, higher elevation and all elevation angles in between. Hence, a range of interference

levels are incident to the satellite receiver due to variations in the interference geometries involved.

Because of the large scale of the IMT deployment, the study models and deploys equivalent objects that are representative of many IMT base stations. The study models interference sourced from an IMT network deployed on the surface of the Earth incident to the SRS space station receiver in Visualyse Professional software.

#### 4.4.1 Technical characteristics

##### 4.4.1.1 Technical and operational characteristics of IMT systems operating in the frequency band 6 425-7 125 MHz

In this initial study of interference from IMT into SRS (deep space) [we] consider an IMT deployment which extends over the land area of the Earth's surface, and using characteristics of IMT base stations deployed in urban macro cells. Table 4-4-1 sets out the IMT characteristics used in this study.

TABLE 4-4-1  
IMT characteristics

IMT characteristic	Description/Value
Deployment	Outdoor urban/suburban macro
Unwanted emissions/base station	-13 dBm/MHz
Area of deployment	148,870,000 km <sup>2</sup> (Note 1)
Number of base stations	1,667,344 (Note 2)
Antenna pattern	ITU-R M.2101 outdoor urban
Mechanical downtilt	10 degrees

The IMT network is represented in the software simulations by 2 783 equivalent objects. Unwanted emissions per base station = -13 dBm/MHz, or -43 dBW/MHz, and total unwanted emissions from the entire network calculated via the following formula:

$$P_{earth} = -43 + 10 \cdot \log(1,667,344) = 19.22 \text{ dBW/MHz}$$

The SRS interference criterion is referenced to 20 Hz, hence unwanted emissions from the entire network is  $P_{earth} = -27.77 \text{ dBW/20 Hz}$ . With 2 783 equivalent modelling objects deployed, unwanted emissions per equivalent object = -62.21 dBW/20 Hz.

Table 4-4-2 sets out the SRS satellite characteristics used in this study.

TABLE 4-4-2

**SRS characteristics**

SRS characteristic	Description/Value
Satellite	Mars Express
Satellite orbit	Mars
Inclination	86.3 degrees (Mars orbit)
Range from Earth	54 to 400 million km
Antenna gain (high gain)	48 dBi
Interference protection criterion	-190 dBW/20 Hz

The size of the Earth seen from Mars' close approach is 0.01°. The satellite is equipped with low, medium and high gain antennas, but we assume that the satellite's high gain antenna is pointing towards a station on Earth. Assuming peak gain is applied to signals from all visible base stations for all of the satellite's antennas may be conservative but is the only assumption we can make for the high gain antenna, based on the information provided.

**4.4.2 Methodology**

The calculation we are making is an interference level as seen at the distant victim receiver. The essential elements of the instantaneous calculation can be written as follows:

**Equation 4-4-1**

**Aggregate interference to a very distant interferer**

$$I_{agg} = \sum_{\text{all visible BS}} [P_{BS} + G_{BS}(\theta_{BS \rightarrow victim}) - P_l(\text{range}_{BS \rightarrow victim}) + G_{victim}(\theta_{victim \rightarrow BS})] + \text{network activity factors}$$

$P_{BS}$  is the unwanted emissions at the base station

$G_{BS}(\theta_{BS \rightarrow victim})$  is the base station gain towards the victim

$P_l(\text{range}_{BS \rightarrow victim})$  is the pathloss between the base station and the victim

(this pathloss is calculated using Recommendation ITU-R P.525 (free space))

$G_{victim}(\theta_{victim \rightarrow BS})$  is the gain of the victim towards the base station

The network activity factors are network loading and TDD, however these are not included in this initial study. Most of the factors in the calculation are uncertain or variable in some way, and are independent of each other. However, not all of the variability has an important impact on the calculations in this study.

The study looks at interference seen when Mars is at its closest approach. The orbiter moves around Mars in an elliptical orbit with a semi-major axes of 17,000 km. This number is small in comparison with the theoretical close approach of 54 million km. So we can assume path loss varies by a small amount during the close approach (and at all other times).

---

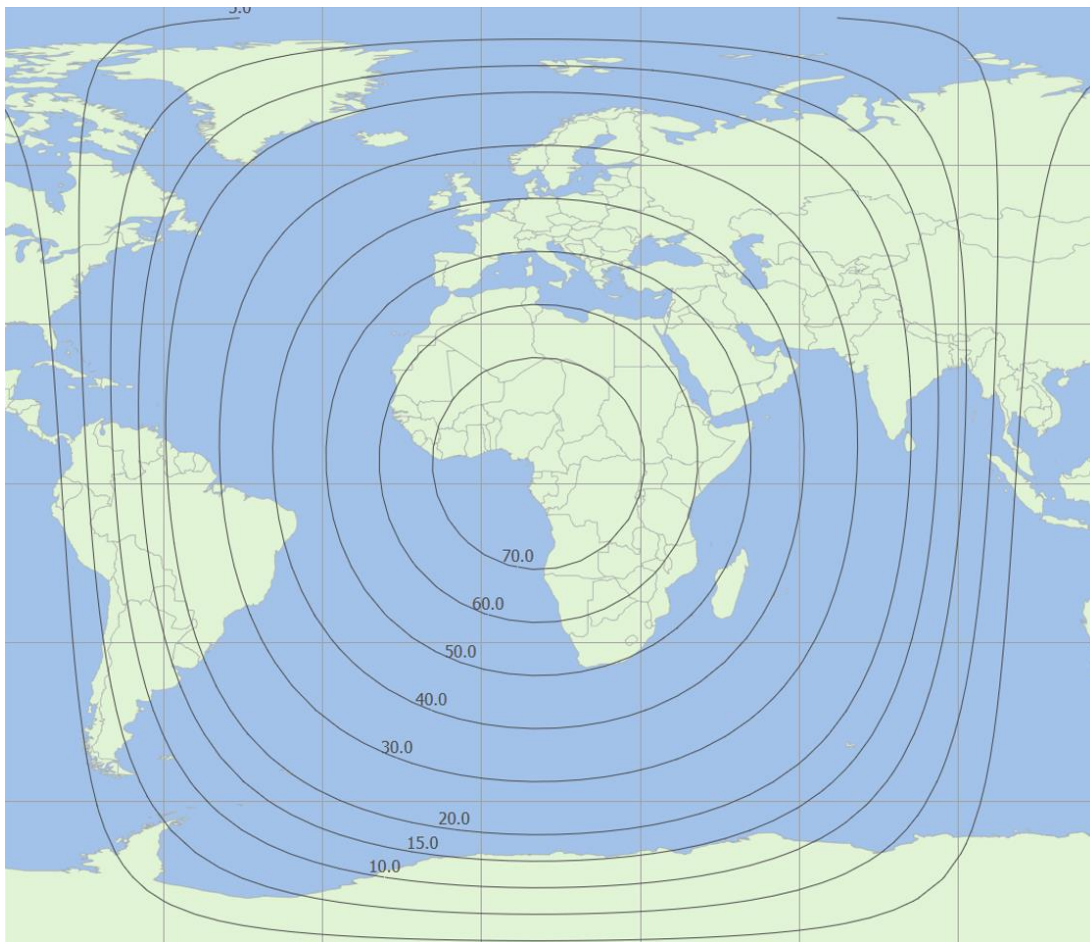
The last Martian close approach was in October 2020 and the minimum distance was more than 62 million km, the next close approach in September 2035 will have a minimum distance of around 57 million km. In this study we use the period around 15 September 2035 as the default date for all of our calculations.

This observation relies on the fact that the calculated azimuth and elevation towards the Mars orbiter will be very similar for points on the surface of the Earth that are close together. This implies some level of pixelation of the Earth's surface such that the difference in pointing angles within a pixel has negligible impact on the calculation of aggregate interference.

Figure 1 below shows the instantaneous elevation of Mars over the surface of the Earth. The contours at low elevation are separated by  $5^\circ$ . When we consider the elevation dependence of the base station antenna gain below, we use a  $5^\circ$  quantisation. When deciding on the size of pixel to use in the analysis below, we ensure that pixels are smaller than the  $5^\circ$  elevation contours. The  $5^\circ$  quantisation is arbitrary but can be tested to make sure it is not too coarse.

FIGURE 4-4-1

**Elevation of Mars as instantaneously seen from Earth**





Consider a general approach to modelling in which the Earth is divided into pixels. We would like the pixels to be sized such that all of the variable and uncertain parameters in Equation 1 are constant within each pixel. If that is the case we can replace  $n$  base stations in the pixel with one equivalent object which has  $10 \cdot \log(n)$  times the unwanted emissions of a single base station. Clearly this is an approximation which will become more accurate as we increase the number of pixels.

Then Equation 4-4-1 becomes

**Equation 4-4-2**  
**Aggregate interference to a very distant interferer from pixel model**

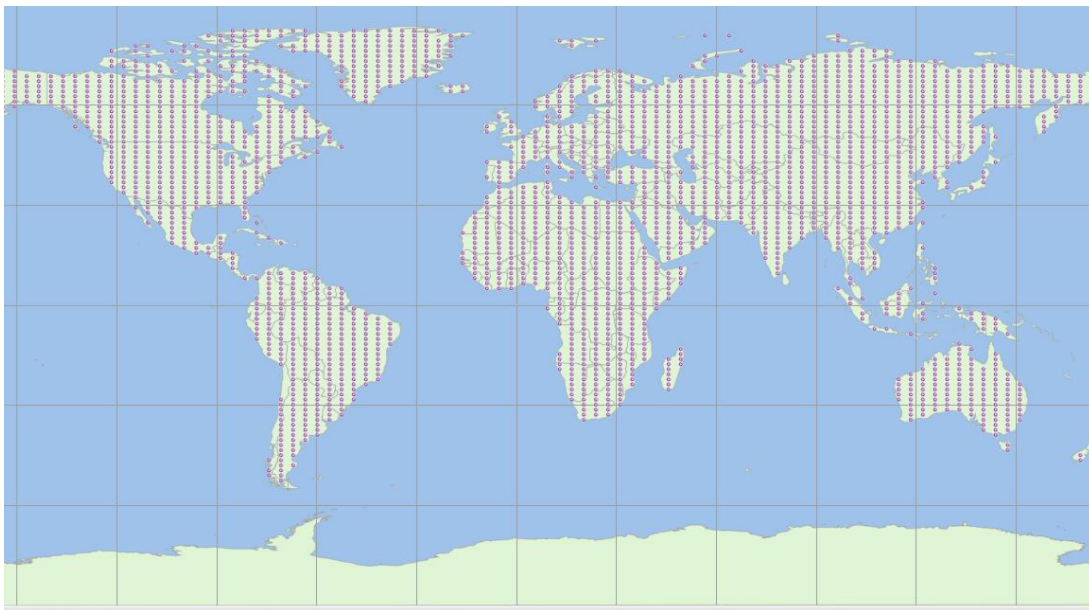
$$I_{agg} = P - P_l + G_{victim} + 10 \cdot \log \sum_{pixels} 10^{(G_{BS}(\theta_{pixel \rightarrow victim})/10)}$$

The only uncertain number in this equation is the base station gain which we assign to each pixel. We have derived a distribution of gain as a function of elevation angle which can be applied to every equivalent object in the simulation.

Our model takes this gain distribution and deploys it over the 2 783 locations shown in Figure 4-4-2. An equivalent object at each location effectively models around 599 base stations. So the total emissions from the land on Earth remains consistent with our earlier calculation.

FIGURE4-4-2

**Base stations represented by 2 783 equivalent objects**



It is possible to derive statistics of gain, as a function of elevation for a single base station, and this is the starting point for the characterisation of the emissions from a pixel containing many base stations.

The model simulates a single base station for an urban macro cell with three hexagonal sectors. Each beam has a  $10^\circ$  mechanical downtilt and is electronically steered to a user terminal placed randomly within the sector, with equal probability across the sector. Antenna gain from an

outdoor urban base station antenna is logged as a function of elevation for 1 million samples. There are multiple possible gain values at each elevation, corresponding to different values of the electronic pointing angle, which is determined by the user terminal location. In our simulation, we have taken the average value of gain in each 5° elevation bin.

The calculations in this study are of an interference level as seen at 200 km orbit. The essential elements of the instantaneous calculation can be written as follows:

**Equation 4-4-3**  
**Aggregate interference to a distant interferer**

$$I_{agg} = \sum_{\text{all visible BS}} [P_{BS} + G_{BS}(\theta_{BS \rightarrow victim}) - P_l(\text{range}_{BS \rightarrow victim}) - P_{clutter}(\text{elvation } BS - victim) + G_{victim}(\theta_{victim \rightarrow BS})] + \text{network activity factors} + \text{TDD factors} + \text{polarisation factors}$$

where:

$P_{BS}$  is the unwanted emissions at the base station;

$G_{BS}(\theta_{BS \rightarrow victim})$  is the base station gain towards the victim;

$P_l(\text{range}_{BS \rightarrow victim})$  is the pathloss between the base station and the victim (this pathloss is calculated using Recommendation ITU-R P.525 (free space));

$P_{clutter}(\text{elvation } BS - victim)$  is the elevation dependent clutter loss calculated as the median loss from Rec. ITU-R P.2108 for a given elevation angle / equivalent object;

$G_{victim}(\theta_{victim \rightarrow BS})$  is the gain of the victim towards the base station.

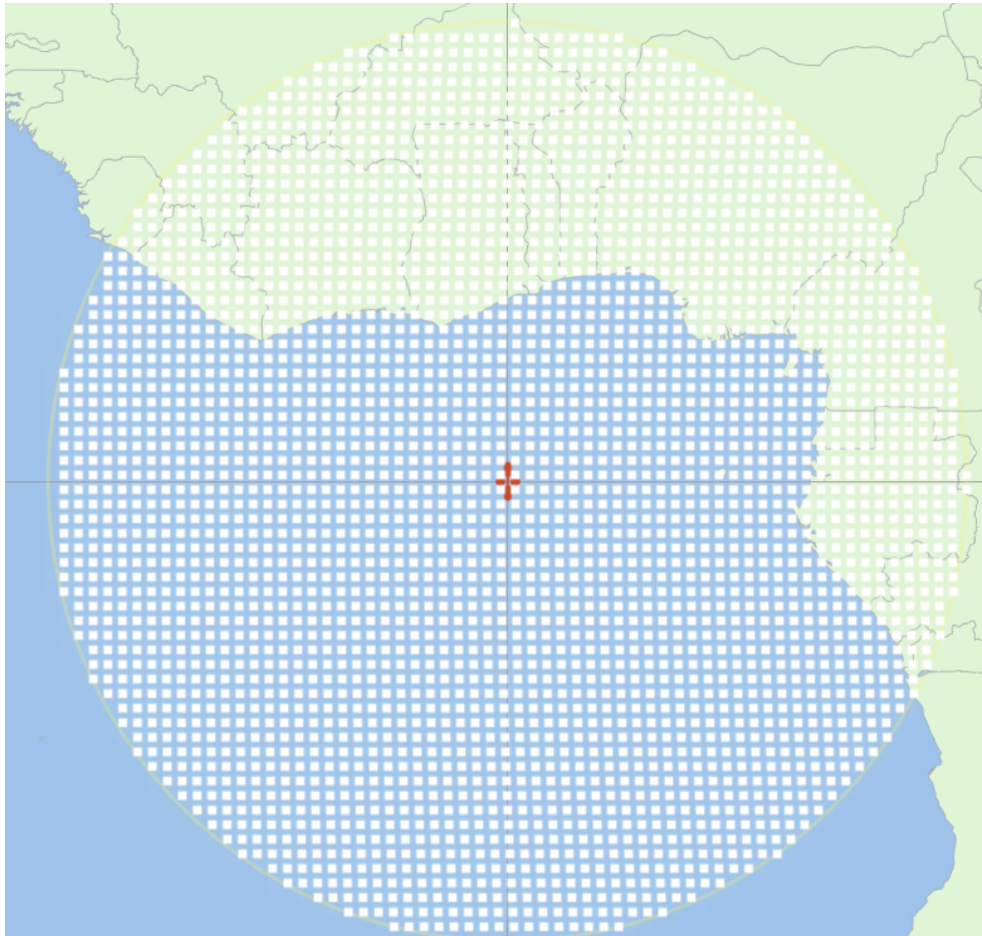
A network loading factor of 20% is included, and a base station TDD activity factor of 75%. This implies a reduction in aggregate EIRP of 6.99 + 1.24 = 8.23 dB. The modelling also includes -3 dB for polarisation mismatch loss – a value that is generally applicable whenever there are a large number of interferers with unknown or variable planes of polarisation.

Consider a general approach to modelling in which the Earth is divided into pixels. The pixels should ideally be sized such that all of the variable and uncertain parameters in Equation 1 are constant within each pixel. If that is the case, n base stations in the pixel can be replaced with one equivalent object which has  $10 \cdot \log(n)$  times the unwanted emissions of a single base station. Clearly this is an approximation which will become more accurate as we increase the number of pixels.

The 3089 equivalent objects in this study imply a separation of equivalent objects of around 50 km. An illustrative deployment is shown in Figure 4-4-3 below. The calculation is independent of satellite location.

FIGURE 4-4-3

**Illustrative deployment**



Then Equation 4-4-1 becomes

**Equation 4-4-4**  
**Aggregate interference from pixel model**

$$I_{agg} = P - P_l + G_{victim} + \text{Activity} + \text{TDD} + \text{Polarisation loss} + 10 \cdot \log \sum_{pixels} - P_{clutter} + 10^{(G_{BS}(\theta_{pixel \rightarrow victim})/10)}$$

The only uncertain numbers in this equation are the base station antenna gain and the elevation dependent clutter loss which are assigned to each pixel. A distribution of BS gain as a function of elevation angle is derived, which can be applied to every equivalent object in the simulation.

The model takes this gain distribution and deploys it over the 3,089 locations. An equivalent object at each location effectively models around 28 base stations. So the total emissions from the land on Earth remains consistent with the earlier calculation.

The calculation is split into two parts, to account for the urban base stations, which make up around 90% of interferers, and the suburban base stations. Although there are far fewer suburban base stations, the suburban case is explicitly modelled separately since the elevation dependence may be less favourable than in the urban case.

It is possible to derive statistics of gain, as a function of elevation for a single base station, by Monte-Carlo simulation, and this has been done for urban and suburban deployments.

This dynamic model simulates a single base station for an urban or suburban macro cell with three hexagonal sectors. Each beam is electronically steered to a user terminal placed randomly within the sector, with equal probability across the sector. Antenna gain from a base station antenna is logged as a function of elevation for 1 million samples. There are multiple possible gain values at each elevation, corresponding to different values of the electronic pointing angle, which is determined by the user terminal location.

Figures 4-4-3 and 4-4-5 below illustrate average (mean) values of gain at each elevation derived from the simulation for the urban and suburban cases respectively.

FIGURE 4-4-4

Average gain vs elevation derived from dynamic simulation - urban case

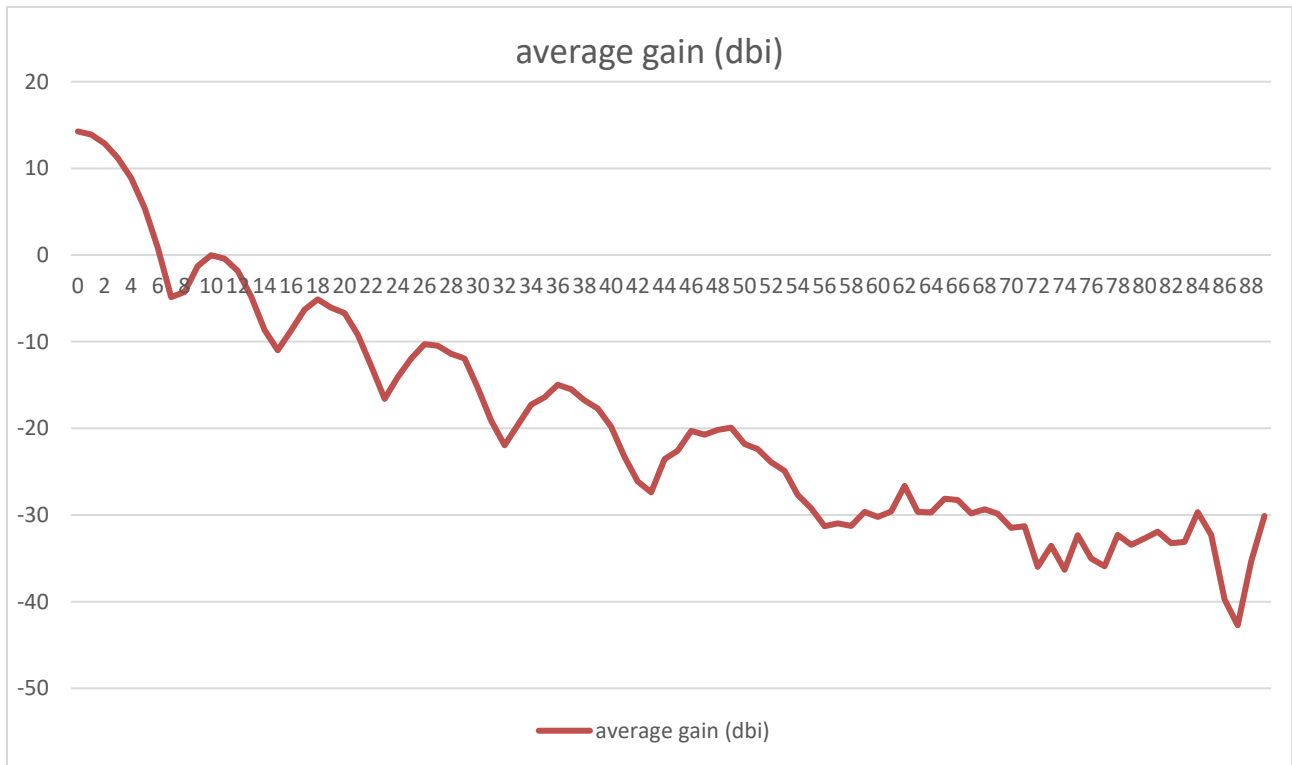
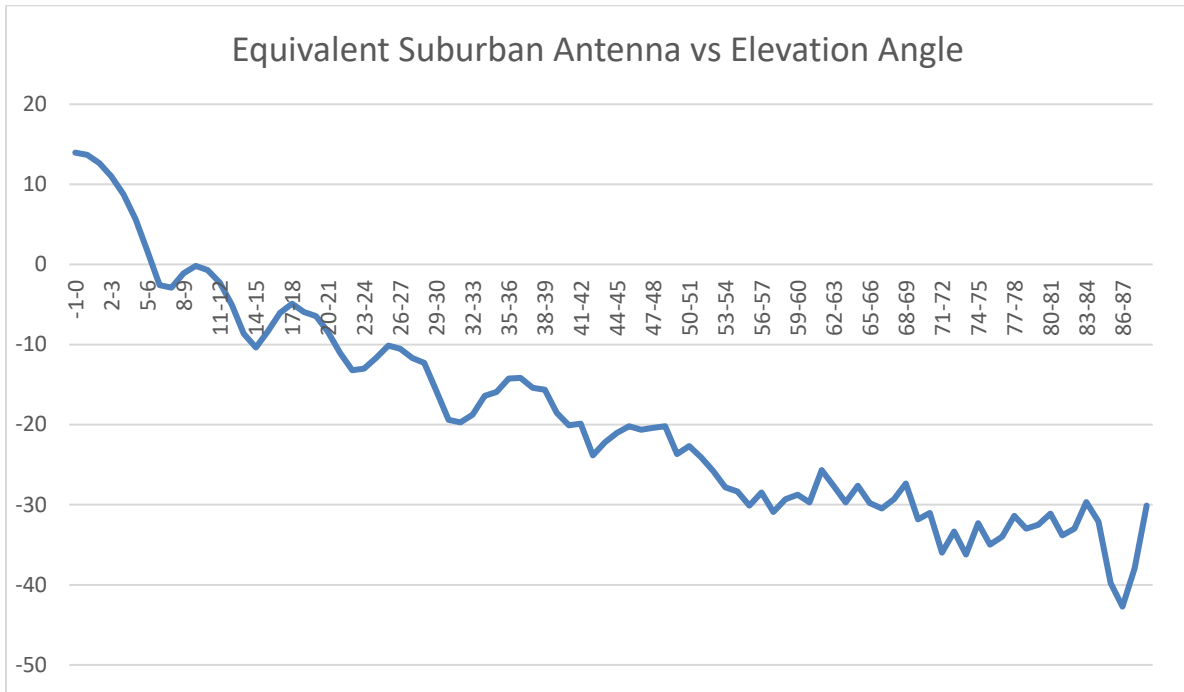


FIGURE 4-4-5

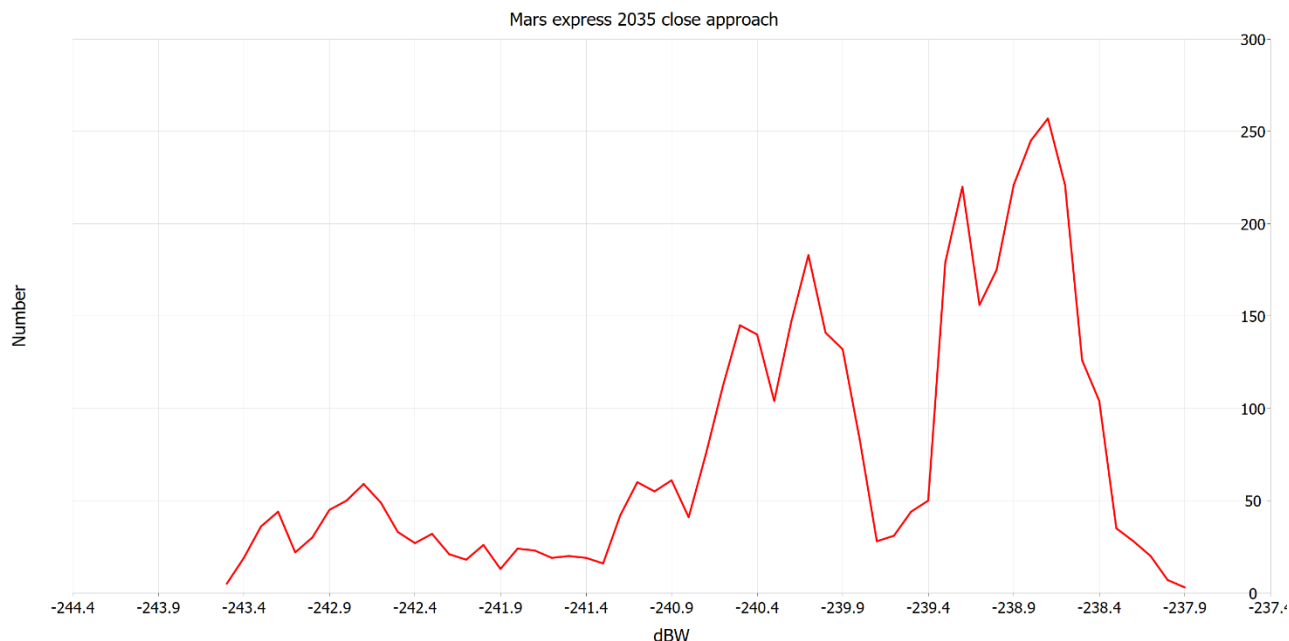
Average gain vs elevation derived from dynamic simulation - suburban case



#### 4.4.3 Study results

The simulation used in this study involves the movement of Earth, Mars and Mars Express over a 24 hour period. Mars Express will see different portions of Earth's surface during this period and so varying levels of aggregate interference from the IMT deployment on Earth. A 24 hour period allows for all possible interference geometries during Mars' closest approach to Earth to be exercised. The value of interference seen by Mars Express will depend on which hemisphere of the Earth is facing Mars. Therefore, we have run a 24 hour simulation in Visualyse Interplanetary. The distribution of  $I_{agg}$  values (dBW/20 Hz) is shown in Figure 4-4-6 below.

FIGURE 4-4-6  
PDF of  $I_{agg}$  (dBW/20 Hz)



We can see from the simulation results that this initial model delivers a very large margin of around 47.9 dB. This provides a clear indication that there is no interference problem for this compatibility scenario. Furthermore, the study is conservative in some aspects and includes some simplifications in the modelling. Additional refinements seem unnecessary to close this case, even though the model could be improved by including factors such as network loading and TDD activity factor, and clutter loss at base station locations. This initial study is sufficient to show that there is no compatibility problem in this case; however, for compatibility scenarios where the margin may be smaller, such simplifications may not be appropriate and all such factors need to be included in the modelling.

The calculation in this study is based on a snapshot analysis of instantaneous interference that may potentially occur for SRS satellites in LEO, LEOP or in the mission return phase. The study assumes an orbit height of 200 km, 0 dB SRS antenna gain and 330K receiver noise temperature and that the satellite footprint is completely filled with IMT base stations.

The simulation returns a single, instantaneous value of aggregate interference  $I$  in 20 Hz of -233.8 dBW/20 Hz, or 43.8dB below the threshold. This value is the sum of contributions from urban (-234.25 dBW/20 Hz) and suburban (-244.04 dBW/20 Hz) base stations.

This result provides a clear indication that there is no interference problem for this compatibility scenario.

#### 4.4.4 Summary and analysis of the results

This section calculates the potential for interference from IMT deployments on the surface of the Earth into an SRS space station receiver, which is assumed to be in deep space and in early/return mission phase / orbit around the Earth. These studies demonstrate that there is no

compatibility problem in both of these cases, with margins of around 48 dB and 44 dB between the aggregate interference and interference protection criteria respectively.

#### 4.5 Sharing and compatibility of the SOS operating in the frequency band 7 100-7 155

This study considers interference from a deployment of IMT networks over the surface of the Earth incident to a victim receiver in the space operation service (SOS) which is in orbit around the Earth.

The study is modelled in Visualyse Professional software. Because of the large scale of the IMT deployment, the study models and deploys equivalent objects that are representative of many IMT base stations.

##### 4.5.1 Technical characteristics

##### 4.5.1.1 Technical and operational characteristics of SOS operating in the frequency band 7100-7155 MHz

Table 3 sets out the relevant characteristics of the SOS uplink used in this study and Figures 1 and 2 show the SOS antenna characteristics specified in the simulation.

TABLE 4-5-1

**Characteristics of the SOS uplink**

Representative orbits	System C
<b>Orbit description</b>	
Type of orbit	Low-Earth, elliptical
Orbit altitude (km)	200-450
Inclination (°)	70
<b>Earth station</b>	
Location	Centre of IMT deployment
Power range at antenna input (dBW)	-14 to -34 (Mode 1) -3 to -23 (Mode 2)
Antenna diameter (m)	5
Antenna gain (dBi)	47
Antenna pattern	Rec. ITU-R S.465
Implied antenna efficiency	0.37
Minimum elevation angle (°)	5
Max e.i.r.p. range (dBW)	33 / 13 (Mode 1) 44 / 24 (Mode 2)
Uplink signal	Telemetry, tracking and telecommand

Necessary bandwidth (MHz)	1.2
<b>Space station</b>	
a) Low gain antenna (dBi)	+1 (Mode 2) *
b) High gain antenna (dBi)	+12 (Mode 1) **
System noise temperature (°K)	1000

\* Mode 1 – Operation involving a narrow-beam space-borne antenna (see Fig. 2).

\*\* Mode 2 – Operation involving a wide-beam space-borne antenna (see Fig. 3).

FIGURE 4-5-1

**Mode 1 antenna pattern**

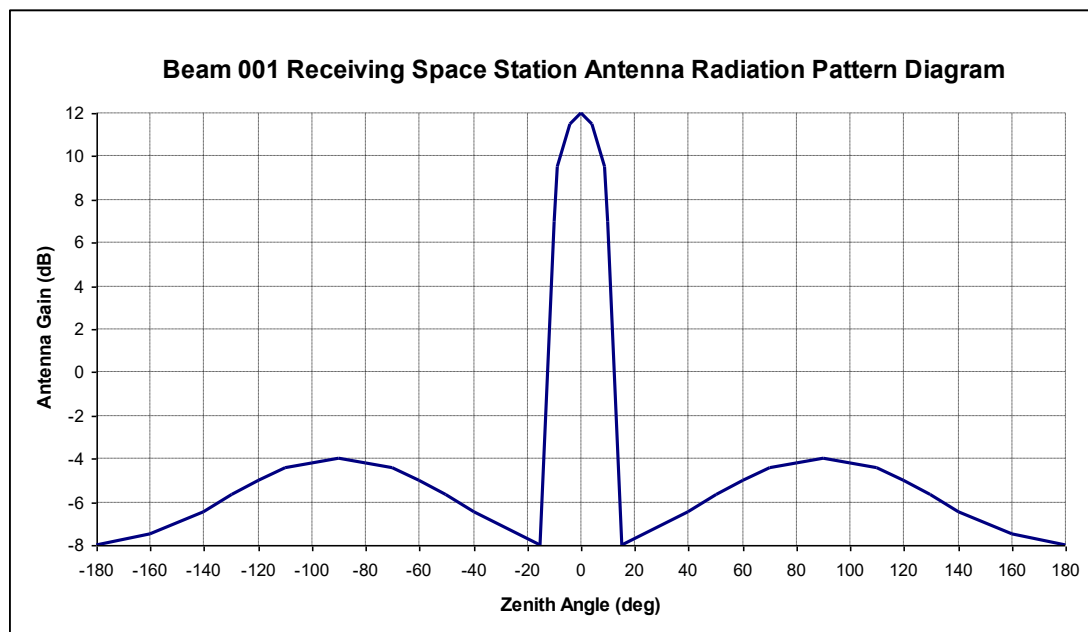
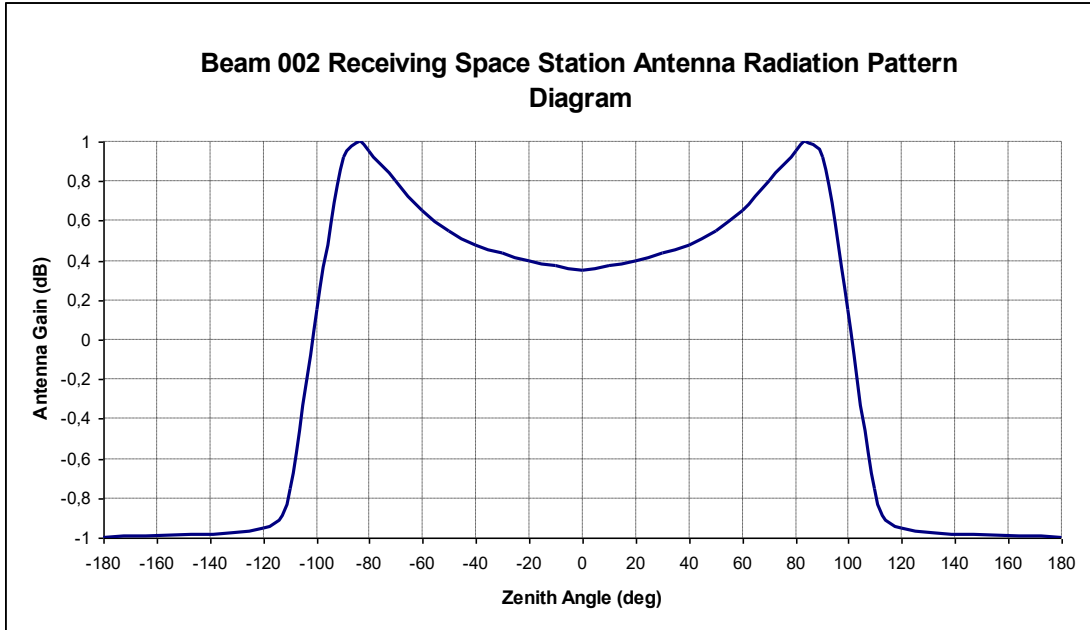




FIGURE 4-5-2

**Mode 2 antenna pattern**



For both Mode 1 and Mode 2 operations, the wanted power level at the satellite receiver is set at  $-161.6$  dBW/kHz, assuming that adaptive power control is able to deliver a practical  $C/N = 7$  dB objective.

**4.5.2 Methodology**

The study calculates  $C/I$  levels seen at the SOS satellite receiver in 1 kHz for an extensive sample of interference geometries given by the satellite's orbital parameters and an equivalent model of the IMT network.

The study involves a Monte Carlo simulation where the satellite location varies over 10,000 instances within an orbit shell defined by a height range of 200 - 450 km and latitude and longitude ranges of 30 degrees. The  $C/I$  calculation is repeated for Mode 1 and Mode 2 antennas on the satellite which are directed towards the SOS earth station at the centre of the IMT deployment. The Monte Carlo simulation is not specific to any particular region of the Earth but is a search for worst-case interference scenarios and the  $C/I$  ratios available. This is based on the SOS satellite's characteristics including its orbital parameters and a large scale IMT deployment.

When calculating aggregate interference incident to the satellite receiver a network loading factor of 20% and a TDD activity factor of 75% are exercised. For the interference calculations the network loading factor expressed in decibels is given by:

$$F_{net} = 10 \cdot \log \log \left( \frac{p_{net}}{100} \right) \quad (\text{dB})$$

where  $p_{net}$  is network loading expressed as the percentage of base stations simultaneously active across the IMT networks. The TDD activity factor is also expressed in decibels:

$$F_{TDD} = 10 \cdot \log \log \left( \frac{p_{TDD}}{100} \right) \quad (\text{dB})$$

where  $p_{TDD}$  is TDD activity factor expressed as the percentage of active base stations transmitting. Therefore,  $F_{net} = -7$  dB and  $F_{TDD} = -1.2$  dB are calculated.

The study also accounts for a 3-dB polarisation mismatch loss on the interference path.

Equation (6) calculates interference incident to the satellite receiver from one equivalent object:

$$I_{equiv} = P_{con}^{equiv(dep)} + G_{\theta}^{equiv(dep)} - L_{clutt} - L_{path} - L_{pol} - F_{net} - F_{TDD} + G_{\phi}^{sat} \quad (\text{dBW/kHz})$$

$I_{equiv}$ : interference at the satellite receiver from one equivalent object (dBW/kHz)

$P_{con}^{equiv(dep)}$ : conducted power per equivalent object for a deployment type (dBW/kHz)

$G_{\theta}^{equiv(dep)}$ : equivalent object antenna gain towards the satellite for a deployment type (dBi)

$L_{clutt}$ : clutter loss at the equivalent object location (dB)

$L_{path}$ : path loss (dB)

$L_{pol}$ : polarisation mismatch loss (dB)

$F_{net}$ : network loading factor (dB)

$F_{TDD}$ : TDD activity factor (dB)

$G_{\phi}^{sat}$ : satellite antenna gain towards the interfering object (dBi)

Clutter loss  $L_{clutt}$  is calculated using the Earth-space statistical clutter loss model specified in section 3.3 of Recommendation ITU-R P.2108 with loss calculated using a value not exceeded for 50% of locations.

$L_{path}$  is calculated using the free space path loss model specified in Recommendation ITU-R P.525.

For  $G_{\theta}^{equiv(dep)}$  distributions of IMT base station antenna gain are derived as a function of elevation angle which can be applied to the urban or suburban macro equivalent objects in the simulation.

It is possible to derive statistics of antenna gain as a function of elevation for a single base station and this is the starting point for the characterisation of the emissions from an equivalent object representing many base stations.

In order to build antenna patterns for the equivalent objects supplementary simulations were developed where a dynamic model simulates an urban macro or suburban macro cell with three hexagonal sectors. Each beam has a mechanical downtilt (6° suburban, 10° urban) and is electronically steered to a user terminal placed randomly within the sector, with equal probability

across the sector. Antenna gain from an outdoor base station antenna is logged as a function of elevation for 1 million samples. There are multiple possible gain values at each elevation, corresponding to different values of the electronic pointing angle, which is determined by the user terminal location. In the simulation, the average value of gain for each degree of elevation is taken.

While an equivalent object must include an antenna model that characterises base station antenna gain at all azimuths based on calculated elevation angles towards the SOS satellite receiver, the underlying interference model rests on aggregation of interference from many base station sectors, where each base station contributes interference from one base station sector in a 3 sector cell.

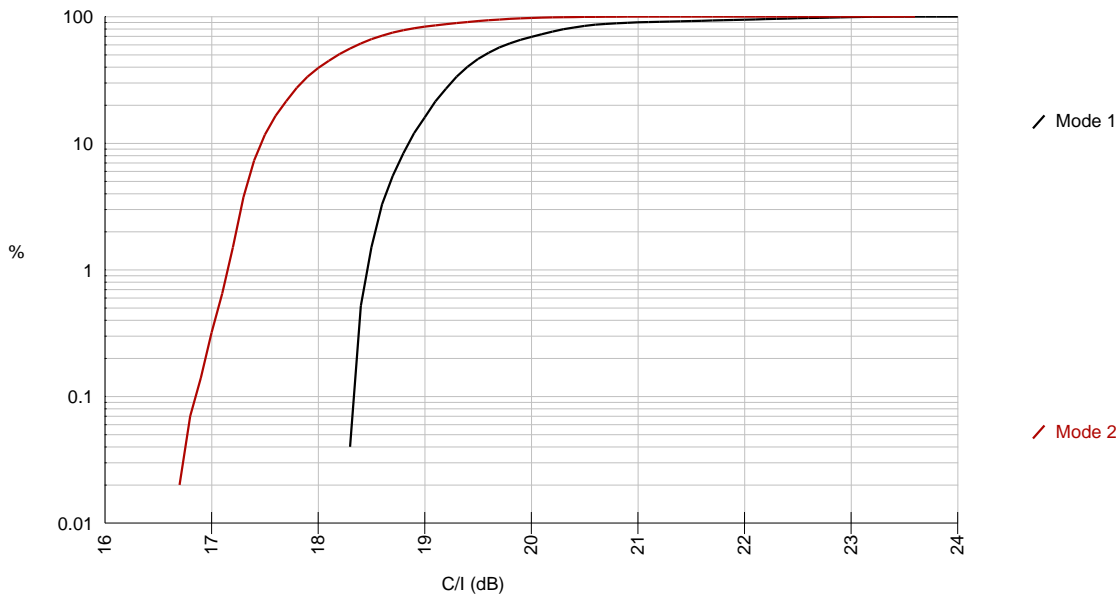
Equation (7) calculates aggregate interference at the satellite receiver at each step in the simulations and is the summation of interfering signals from all equivalent objects:

$$\Sigma I_{equiv} = 10 \cdot \sum 10^{\frac{I_{equiv}}{10}} \quad (dBW/kHz)$$

### 4.5.3 Study results

The calculations in this study are based on a Monte Carlo simulation of interference geometry which constitutes an extensive search for worst-case interference scenarios. The output is a statistical distribution of  $C/I$  at the satellite receiver consistent with the orbital parameters available. Figure 4-5-3 shows the cumulative distributions with results for both Mode 1 and Mode 2 operations.

FIGURE 4-5-3  
**C/I distributions**



The results can reliably indicate a range of  $C/I$  values that are possible when the SOS wanted link is configured to support a  $C/N = 7$  dB at the SOS satellite receiver.

Results from this Monte Carlo study are not easily compared against an interference protection criterion which is designed to be tested in the time domain, but it is possible to make general observations. This study has considered an interference problem where the wanted signal level at the SOS satellite receiver delivers  $C/N = 7$  dB exactly and reports on the consequent  $C/I$  ratios in the first instance. However, the transmitter at the SOS earth station utilises power control and there is scope to increase e.i.r.p. as discussed in Recommendation ITU-R SA.365 which states:

*The power of earth station transmitters can generally be increased within the limits imposed by the RR and on-board receivers therefore do not always operate at maximum sensitivity. In particular, for communication with low-altitude satellites operating close to sources of interference from terrestrial services, the transmitted power of earth stations can be kept as high as for geostationary satellites for example, in order to keep an adequate signal-to-interference ratio.*

On this basis, the worst-case  $C/I$  values obtained in the simulation are investigated and the scope for e.i.r.p. uplift at the SOS earth station.

Table 4 shows the potential for e.i.r.p. uplift at the SOS earth station for the worst-case scenarios. Obtaining the wanted path lengths for these scenarios, the e.i.r.p. required in order to satisfy a  $C/N = 7$  dB exactly is calculated. In both cases, the worst-case  $C/I$  values obtained are associated with a small percentage of steps executed in the Monte-Carlo simulation (0.04% for Mode 1 and 0.02% for Mode 2). The simulation is not in the time domain and the results are not compared directly with a  $C/I$  associated with 1% of time.

The study then calculates the scope for e.i.r.p. uplift in these scenarios based on the maximum e.i.r.p. available at the SOS earth station. It can be seen that in both of these worst-case scenarios an e.i.r.p. uplift that delivers  $C/I = 20$  dB is possible. For the Mode 1 case,  $C/I = 20$  dB is achievable with a 1.7 dB uplift with potential for a further 7.7 dB of uplift. In the Mode 2 case,  $C/I = 20$  dB is achievable with a 3.3 dB uplift and with potential for a further 15.9 dB of uplift.

TABLE 4-5-2

**Worst case analysis**

<b>Mode 1</b>	
Worst $C/I$	18.3 dB
Wanted path length	703 km
Path loss	166.4 dB
e.i.r.p. (SOS earth station)	23.6 dBW/1.2 MHz
Scope for e.i.r.p. uplift	+9.4 dB (33 – 23.6)
Scope for further e.i.r.p. uplift after $C/I = 20$ dB is satisfied	+7.7 dB (33 – 23.6 – 1.7)
<b>Mode 2</b>	
Worst $C/I$	16.7 dB

---

Wanted path length	228 km
Path loss	156.6 dB
e.i.r.p. (SOS earth station)	24.8 dBW/1.2 MHz
Scope for e.i.r.p. uplift	+19.2 dB (44 – 24.8)
Scope for further e.i.r.p. uplift after $C/I = 20$ dB is satisfied	+15.9 dB (44 – 24.8 – 3.3)

#### 4.5.4 Summary and analysis of the results

The study concludes that the simulations and analysis indicate that the worst-case scenarios found in an extensive search of interference geometries for both Mode 1 and Mode 2 operations supporting a  $C/N = 7$  dB at the SOS satellite receiver have scope for e.i.r.p. uplifts in order to secure  $C/I = 20$  dB. Therefore, the results of these simulations indicate that for all of the 20 000 interference scenarios tested (10 000 simulation steps with Mode 1 and Mode 2 scenarios considered at each step), a  $C/I = 20$  dB is achievable, and that therefore there is no coexistence problem.

---

---

## 5 Main Discussion and Conclusion

### 5.1 Discussion

In the cycle of WRC-23, many studies have been submitted to WP5D AI 1.2 6GHz study, which indicate that in fact IMT deployments are possible in this band and these can coexist with satellite uplink/downlink, microwave, SOS and SRS. Moreover there are still lots of working assumption are not involved in the ITU studies, which are listed as below,

Coexistence with Fixed Satellite Services:

- Based on the predictions presented in ITU-R, previous experience of a similar study in the 26 GHz band showed that in practice deployment rate was much lower compared to the assumptions made in ITU-R. The 6425–7125 MHz band 5G most likely will have a lower deployment rate compared to the predictions used in the study. It should be also noted, that the study assumed all countries within the satellite footprint implement 5G in the 6 GHz band, however, while the majority of these countries have plans for 5G in the 6 GHz, in practice not all of them may have plans to utilize this band for 5G, and thus the deployment density may be also lower. Since the study showed compatibility for the highest estimated deployment rate, for the lower deployment rate which will most likely be in practice, the compatibility situation will be even better.
- As spectrum in the 3400-4800 MHz range is being progressively assigned for mobile operators use, the use of the same frequencies for FSS is being decreased in many countries and ceased in others. Correspondingly, given the FSS DL and UL pairings, the FSS uplink usage in the 6 GHz range is expected to decrease over time. The coexistence studies considers potential IMT co-existence issues based on current satellite deployment. However, it is also noted that any potential IMT coexistence conditions are likely to become less restrictive over time due to the expected gradually decreasing use of the band by FSS; e.g. due to the corresponding 5G take-up in the paired C-band (FSS downlink) and due to increased use of the Ku/Ka bands.
- In the context of sharing between IMT and FSS uplink in the 6 425-7 025 MHz band, it is considered that technical conditions on the e.i.r.p. of IMT BSs as a function of vertical (elevation) and horizontal (azimuth) angles is preferable to technical conditions on the in-band TRP of IMT BSs. This is because limits on the in-band TRP can result in technical conditions that are unduly restrictive, and not only impact the levels of radiation from IMT BSs towards satellites, but also towards served IMT user equipment and thereby degrade the performance of IMT networks.
  - Importantly, in this contribution we demonstrate that any specified technical conditions on the e.i.r.p. of IMT BSs need only be specified as a function of vertical (elevation) angle, without reference to the horizontal (azimuth) angle. This is because the total interference experienced by a satellite receiver is the aggregate of interference from the IMT BS deployments over large areas on the Earth, where each IMT BS sees the satellite at a deterministic elevation depending on BS's location, but at a uniformly distributed random horizontal angle depending on the horizontal boresight of the BS, which itself depends on IMT network planning constraints and is independent of the location of the satellite.
  - The implication is that the technical conditions on the e.i.r.p. of an IMT BS need only be specified as a function of the vertical (elevation) angle based on the expected value of e.i.r.p. calculated over horizontal (azimuth) angles as well as the relevant beamforming angles, as the IMT BS serves its UEs in both the azimuth (horizontal scan) and elevation (vertical down-tilt) domains. In WRC-23 meeting, an expected e.i.r.p. mask to protect FSS (E-s) was successfully included in the associated Resolution.

---

### Coexistence with Fixed Services:

- Since multiple antenna elements are combined together to form a “logical” element, i.e., a sub-array, the radiation pattern of the “logical” element becomes narrower as compared to the single element case. This can additionally help in reducing the side lobe levels. Furthermore, sub-arrays are designed with an electrical down tilt so that the sub array beam is focussed towards the intended terrestrial users. Thus, while grating lobes may occur due to the sparse arrays (where sub-array spacing  $> 0.5 \lambda$ ) depending on the steering angle, the downtilt can mitigate the impact of the grating lobes.
- For the sub-array configuration, the average gain towards the horizon is lower because the main beam is narrower due to larger aperture size, thereby decreasing the emissions towards the horizon.

### Coexistence with SOS

- One of the studies mentioned that as allocation to SOS is only for an administration specified in RR No. 5.459 and where the communicating earth station is on the administration’s territory (according to Table 3 of doc. 5D/1091), it is therefore necessary to note that protection criteria should be applied during the time periods when the satellite is in operation and can be seen from the administration’s territory.

## 5.2 Conclusion

Based on the study report, sharing and compatibility is possible in the band of 6GHz. Satellite uplink service was highlighted as the main issue. However according to the study in WP5D, IMT deployments are possible in this band and these can coexist with satellite uplink. There are other primary services which are satellite downlink and fixed links, but these are more of a national issue. There can be coordination on a case-by-case basis mainly considering geographical separation.

The 6425-7125 MHz makes sense to be considered for licensed moving forward, in line with the WRC.23 agenda item. It’s an important extension to mid band operation particularly for outdoor urban areas and supporting 5G advanced services moving forward. In terms of the regional specific requirements, if there is harmonization across all regions, that make things simpler from device perspective.

The possibility for the future 6 GHz deployments to exploit 700 MHz of contiguous spectrum while reusing the available mid band site grid allowing citywide outdoor high-capacity coverage.



---

## 6 Abbreviation

DOU	Discharge Of Usage
FDD	Frequency Division Duplex
FS	Fixed Service
FSS	Fixed Satellite Service
GSA	Global mobile Suppliers Association
GSMA	GSM Association
GSO	GeoSynchronous Orbit
I/N	Interference-to-Noise
IMT	International Mobile Telecommunications
ITU-R	International Telecommunication Union-Radio
SOS	Space Operation Service
SRS	Space Research Service
TDD	Time Division Duplex
U6G	Upper 6GHz spectrum
WRC23	2023 World Radiocommunication Conference
XR	Extended reality

---

## 7 References

[1] Ericsson Mobility Report. <https://www.ericsson.com/en/reports-and-papers/mobility-report>

[2] GTI: "GTI White Paper on Future Spectrum Demand of 6GHz Band". Available at <https://www.gtigroup.org/Uploads/File/2022/04/15/u62594643039f8.pdf>

[3] R19-WP5D-230612-TD-0875!R1!MSW-E

[4] R19-WP5D-230612-TD-0876!!MSW-E

[5] R19-WP5D-230612-TD-0877!!MSW-E

[6] R19-WP5D-230612-TD-0878!R1!MSW-E

[7] R19-WP5D-230612-TD-0879!R1!MSW-E

[8] R19-WP5D-230612-TD-0880!R1!MSW-E